Golden Space–Time Trellis Coded Modulation

Yi Hong, *Member, IEEE*, Emanuele Viterbo, *Senior Member, IEEE*, and Jean-Claude Belfiore, *Member, IEEE*

***Abstract*—In this paper, we present a multidimensional trellis coded modulation scheme for a high rate 2×2 multiple-input multiple-output (MIMO) system over slow fading channels. Set partitioning of the Golden code is designed specifically to increase the minimum determinant. The branches of the outer trellis code are labeled with these partitions and Viterbi algorithm is applied for trellis decoding. In order to compute the branch metrics, a sphere decoder is used. The general framework for code design and optimization is given. Performance of the proposed scheme is evaluated by simulation and it is shown that it achieves significant performance gains over the uncoded Golden code.**

***Index Terms*—Coding gain, diversity, Golden code, lattice, minimum determinant, set partitioning, trellis coded modulation.**

I. Introduction

SPACE–TIME codes were proposed in [1] as a combination of channel coding with transmit diversity techniques in order to enhance data rates and reliability in multiple-antenna wireless communications systems. In the coherent scenario, where the channel state information (CSI) is available at the receiver, the design criteria based on *rank* and *determinant criteria* for space–time codes in slow fading channels were developed [1]. The design criteria aim to maximizing the minimum rank and determinant of the codeword distance matrix in order to maximize the diversity and coding gain. This in turn guarantees the best possible asymptotic slope of the error performance curve on a log-log scale, as well as a shift to the left of the curve.

Subsequent work designed new space–time trellis codes and orthogonal space–time block codes [2], [4]. In particular, orthogonal space–time block codes attracted a lot of interest due to their low decoding complexity and high diversity gain. Further work produced full diversity, full rate algebraic space–time block codes for any number of transmit antennas, using number-theoretical methods [5]–[7]. A general family of full rank and full rate linear dispersion space–time block codes based on cyclic division algebras was proposed in [8]. However, all the above coding schemes did not always exploit the full potential of the multiple-input multiple-output (MIMO) system in terms of diversity–multiplexing gain tradeoff [3]. In [9], the Golden code was proposed as a full rate and full diversity code for 2×2 MIMO systems with nonvanishing minimum determinant (NVD). It was shown in [10] how this property guarantees the achievement of the diversity–multiplexing gain tradeoff.

In this work, we focus on the slow-fading model, where it is assumed that the channel coefficients are fixed over the duration of a fairly long frame. In such a case, in order to reduce the decoding complexity, concatenated coding schemes are appropriate. Space–time trellis codes (STTCs) transmitting phase-shift keying (PSK) or quadrature amplitude modulation (QAM) symbols from each antenna were designed according to both *rank* and *determinant* criteria [1]. A more flexible design, using a concatenated scheme, enables to separate the optimization of the two design criteria. As an inner code, we can use a simple space–time block code, which can guarantee full diversity for any spectral efficiency (e.g., Alamouti code [2]). An outer code is then used to improve the coding gain. Essentially two approaches are available:

- bit-interleaved coded modulation (BICM) using a powerful binary code and computing bit reliability (soft outputs) for the inner code;
- trellis-coded modulation (TCM) using set partitioning of the inner code.

The first approach requires a soft-output decoder of the inner code, which can have high complexity as the spectral efficiency increases. The second approach, considered in this paper, overcomes the above limitations and is appropriate for high data rate systems. We note how the NVD property for the inner code is essential when using a TCM scheme: such schemes usually require a constellation expansion, which will not suffer from a reduction of the minimum determinant. This advantage is not available with super-orthogonal STTCs proposed in [12].

A first attempt to concatenate the Golden code with an outer trellis code was made in [18]. Set partitioning of the inner code was used to increase the minimum determinant of the inner codewords, which label the branches of the outer trellis code. The resulting *ad hoc* scheme suffered from a high trellis complexity.

In this paper, we develop general framework for code design and optimization for Golden space–time trellis coded modulation (GST-TCM) schemes. In [13]–[16], lattice set partitioning, combined with a trellis code, is used to increase the minimum square Euclidean distance between codewords. Here, it is used

Manuscript received April 14, 2006; revised December 5, 2006. This work was supported by the STREP Project IST-026905 (MASCOT) within the Sixth Framework Programme of the European Commission, ARC under Grant DP0663567, and ACoRN under Grant RN0459498. This work was presented in part at the 2006 International Symposium on Information Theory and its Applications, Seoul, Korea, October 2006 and the Joint Workshop of Network of Excellence in Wireless Communications (NEWCOM) and Australian Research Council (ARC) Communications Research Network (ACoRN), Vienna, Austria, September 2006.

Y. Hong is with the Institute for Telecommunications Research, University of South Australia, SPRI Building, Mawson Lakes SA 5095, Australia (e-mail: yi.hong@unisa.edu.au).

E. Viterbo was with Politecnico di Torino, Italy. He is now with D.E.I.S., Università della Calabria, 87036 Rende (CS), Italy (e-mail: viterbo@deis.unical.it).

J.-C. Belfiore is with the Department of Communications and Electronics, École Nationale Supérieure des Télécommunications, 75013, Paris, France (e-mail: belfiore@enst.fr).

Communicated by Ø. Ytrehus, Asspciate Editor for Coding Techniques.

Color versions of Figures 3, 4, 8–15, 17, and 18 are available online at http://ieeexplore.ieee.org.

Digital Object Identifier 10.1109/TIT.2007.894626

0018-9448/$25.00 © 2007 IEEE

Authorized licensed use limited to: University of South Australia. Downloaded on November 23, 2008 at 22:42 from IEEE Xplore. Restrictions apply.

to increase the minimum determinant. The Viterbi algorithm is used for trellis decoding, where the branch metrics are computed by using a lattice sphere decoder [11] for the inner code.

We consider partitions of the Golden code with increasing minimum determinant. In turn, this corresponds to a $\mathbb{Z}^8$ lattice partition, which is labeled by using a sequence of nested binary codes. The resulting partitions are selected according to a design criterion that is similar to Ungerboeck design rules [14], [19]. We design different GST-TCMs and optimize their performance according to the design criterion.

For example, we will show that 4- and 16-state TCMs achieve significant performance gains of 3 and 4.2 dB, at frame error rate (FER) of 10^{-3}, over the uncoded Golden code at spectral efficiencies of 7 and 6 bits per channel use (bpcu), respectively.

The rest of the paper is organized as follows. Section II introduces the system model. Section III presents a set partitioning of the Golden code which increases the minimum determinant. Section IV, the GST-TCM, presents design criteria and various examples of our scheme. Conclusions are drawn in Section V.

The following notations are used in the paper. Let T denote transpose and $\dagger$ denote Hermitian transpose. Let $\mathbb{Z}, \mathbb{Q}, \mathbb{C}$, and $\mathbb{Z}[i]$ denote the ring of rational integers, the field of rational numbers, the field of complex numbers, and the ring of Gaussian integers, where $i^2 = -1$. Let GF(2) $= \{0, 1\}$ denote the binary Galois field. Let $\mathbb{Q}(\theta)$ denote an algebraic number field generated by the primitive element θ. The real and imaginary parts of a complex number are denoted by $\Re(\cdot)$ and $\Im(\cdot)$. The $m \times m$-dimensional identity matrix is denoted by $\boldsymbol{I}_m$. The $m \times n$-dimensional zero matrix is denoted by $\mathbf{0}_{m\times n}$. The Frobenius norm of a matrix is denoted by $\|\cdot\|_F$. Let $\mathbb{Z}^8$ be the eight-dimensional integer lattice and let D_4 and E_8 (Gosset lattice) denote the densest sphere packing in four and eight dimensions [21].

II. System Model

We consider a 2×2 ($n_T = 2, n_R = 2$) MIMO system over slow-fading channels. The received signal matrix $\boldsymbol{Y} \in \mathbb{C}^{2\times 2L}$, where $2L$ is the *frame* length, is given by

$$\boldsymbol{Y} = \boldsymbol{H}\boldsymbol{X} + \boldsymbol{Z} \tag{1}$$

where $\boldsymbol{Z} \in \mathbb{C}^{2\times 2L}$ is the complex white Gaussian noise with independent and identically distributed (i.i.d.) samples $\sim\mathcal{N}_{\mathbb{C}}(0, N_0)$, $\boldsymbol{H} \in \mathbb{C}^{2\times 2}$ is the channel matrix, which is constant during a frame and varies independently from one frame to another. The elements of $\boldsymbol{H}$ are assumed to be i.i.d. circularly symmetric Gaussian random variables $\sim \mathcal{N}_{\mathbb{C}}(0, 1)$. The channel is assumed to be known at the receiver.

In (1), $\boldsymbol{X} = [X_1, \ldots, X_t, \ldots, X_L] \in \mathbb{C}^{2\times 2L}$ is the transmitted signal matrix, where $X_t \in \mathbb{C}^{2\times 2}$. There are three different options for selecting inner codewords $X_t, t = 1, \ldots, L$.

1) X_t is a codeword of the Golden code $\mathcal{G}$, i.e.,

$$X_t = \frac{1}{\sqrt{5}}\begin{bmatrix} \alpha(a+b\theta) & \alpha(c+d\theta) \\ i\bar{\alpha}(c+d\bar{\theta}) & \bar{\alpha}(a+b\bar{\theta}) \end{bmatrix} \tag{2}$$

where $a, b, c, d \in \mathbb{Z}[i]$ are the information symbols, $\theta = 1-\bar{\theta} = (1+\sqrt{\frac{5}{2}}), \alpha = 1+i-i\theta, \bar{\alpha} = 1+i(1-\bar{\theta})$, and the factor $\frac{1}{\sqrt{5}}$ is necessary for energy normalizing purposes [9].

2) X_t are independently selected from a linear subcode of the Golden code.
3) A trellis code is used as the outer code encoding across the symbols X_t, selected from partitions of $\mathcal{G}$.

We denote Case 1 as the *uncoded Golden code*, Case 2 as the *Golden subcode*, and Case 3 as the *Golden space–time trellis coded modulation*.

In this paper, we use Q-QAM constellations as information symbols in (2), where $Q = 2^\eta$. We assume the constellation is scaled to match $\mathbb{Z}[i] + (1+i)/2$, i.e., the minimum Euclidean distance is set to 1 and it is centered at the origin. For example, the average energy is $E_s = 0.5, 1.5, 2.5, 5, 10.5$ for $Q = 4, 8, 16, 32, 64$. Without loss of generality, we will neglect the translation vector $(1+i)/2$ and assume the Q-QAM constellation is carved from $\mathbb{Z}[i]$, using a square (or cross-shaped) bounding region $\mathcal{B}_{\mathrm{QAM}}$, typical for QAMs. For convenience in our analysis, we will choose $\mathcal{B}_{\mathrm{QAM}}$ to be in the positive quadrant. In order to minimize the transmitted energy of this constellation, we center it with by adding a suitable translation.

SNR is defined as $\mathrm{SNR} = n_T E_b/N_0$, where $E_b = E_s/q$ is the energy per bit and q denotes the number of information bits per symbol. We have $N_0 = 2\sigma^2$, where σ^2 is the noise variance per real dimension, which can be adjusted as $\sigma^2 = (n_T E_b/2)10^{(-\mathrm{SNR}/10)}$.

Assuming that a codeword $\boldsymbol{X}$ is transmitted, the maximum-likelihood receiver might decide erroneously in favor of another codeword $\hat{\boldsymbol{X}}$. Let r denote the rank of the *codeword difference matrix* $\boldsymbol{X} - \hat{\boldsymbol{X}}$. Since the Golden code is a full rank code, we have $r = n_T = 2$.

Let $\lambda_j, j = 1, \ldots, r$, be the eigenvalues of the *codeword distance matrix* $\boldsymbol{A} = (\boldsymbol{X} - \hat{\boldsymbol{X}})(\boldsymbol{X} - \hat{\boldsymbol{X}})^\dagger$. Let $\Delta = \prod_{j=1}^{n_T} \lambda_j$ be the determinant of the codeword distance matrix $\boldsymbol{A}$ and $\Delta_{\min}$ be the corresponding *minimum determinant*, which is defined as

$$\Delta_{\min} = \min_{\boldsymbol{X}\neq\hat{\boldsymbol{X}}} \det(\boldsymbol{A}). \tag{3}$$

The pairwise error probability (PWEP) is upper-bounded by

$$P(\boldsymbol{X} \to \hat{\boldsymbol{X}}) \leq (\Delta_{\min})^{-n_R}\left(\frac{E_s}{N_0}\right)^{-n_T n_R} \tag{4}$$

where $n_T n_R$ is the *diversity gain* and $(\Delta_{\min})^{1/n_T}$ is the *coding gain* [1]. In the case of linear codes analyzed in this paper, we can simply consider the all-zero codeword matrix and we have

$$\Delta_{\min} = \min_{\boldsymbol{X}\neq\mathbf{0}_{2\times 2L}} |\det(\boldsymbol{X}\boldsymbol{X}^\dagger)|^2. \tag{5}$$

In order to compare two coding schemes for the $n_T \times n_R$ MIMO system, supporting the same information bit rate, but different minimum determinants ($\Delta_{\min,1}$ and $\Delta_{\min,2}$) and different constellation energies ($E_{s,1}$ and $E_{s,2}$), we define the asymptotic coding gain as

$$\gamma_{as} = \frac{\sqrt[n_R]{\Delta_{\min,1}}/E_{s,1}}{\sqrt[n_R]{\Delta_{\min,2}}/E_{s,2}}. \tag{6}$$

We will only consider the case with $n_R = 2$, which enables to exploit the full power of the Golden code with the minimum number of receive antenna. Adding extra receive antennas can

Authorized licensed use limited to: University of South Australia. Downloaded on November 23, 2008 at 22:42 from IEEE Xplore. Restrictions apply.

increase the receiver diversity and hence performance at the cost of higher complexity.

Performance of both uncoded Golden code (Case 1) and Golden subcode (Case 2) systems can be analyzed for $L = 1$. The Golden code $\mathcal{G}$ has full rate, full rank, and the minimum determinant is $\delta_{\min} = \frac{1}{5}$ [9]; thus, for Case 1, $\Delta_{\min} = \delta_{\min}$. For Case 2, a linear subcode of $\mathcal{G}$ is selected such that $\Delta_{\min} > 1/5$. For GST-TCM (Case 3) we consider $L > 1$ and the minimum determinant can be written as

$$\begin{aligned}\Delta_{\min} &= \min_{\boldsymbol{X}\neq\mathbf{0}_{2\times 2L}} \det(\boldsymbol{X}\boldsymbol{X}^{\dagger}) \\ &= \min_{\boldsymbol{X}\neq\mathbf{0}_{2\times 2L}} \det\left(\sum_{t=1}^{L}(X_t X_t^{\dagger})\right). \end{aligned} \tag{7}$$

A code design criterion attempting to maximize $\Delta_{\min}$ is hard to exploit, due to the nonadditive nature of the determinant metric in (7). Since $X_t X_t^{\dagger}$ are positive definite matrices, we use the following determinant inequality [22]:

$$\Delta_{\min} \geq \min_{\boldsymbol{X}\neq\mathbf{0}_{2\times 2L}} \sum_{t=1}^{L} \det(X_t X_t^{\dagger}) = \Delta'_{\min}. \tag{8}$$

The lower bound $\Delta'_{\min}$ will be adopted as the guideline of our concatenated scheme design. In particular, we will design trellis codes that attempt to maximize $\Delta'_{\min}$, by using set partitioning to increase the number and the magnitude of nonzero terms $\det(X_t X_t^{\dagger})$ in (8).

Note that our design criterion is based on the optimization of an upper bound to the upper bound on the worst case PWEP in (4). Nevertheless, simulation results show that the codes with the largest $\Delta'_{\min}$ always performe better.

III. Uncoded Golden Code and Its Subcodes

In both Cases 1 and 2, the symbols X_t are transmitted independently in each time slot $t = 1, \ldots, L$. The subscript t will be omitted for brevity. We recall below the fundamental properties of the Golden code deriving from its algebraic structure [9].

- Full-rank: the cyclic division algebra structure guarantees that all the codewords have full rank (i.e., nonzero determinant).
- Full-rate: the spectral efficiency is of two Q-QAM information symbols per channel use (i.e., $2\log_2(Q)$ bits/s/Hz) and saturates the two degrees of freedom of the 2×2 MIMO system.
- Cubic shaping: this relates to the cubic shape of the vectorized eight-dimensional constellation and guarantees that no shaping loss is induced by the code, i.e., reduced transmitted energy.
- Nonvanishing determinant for increasing Q-QAM size: this property is derived from the discrete nature of the infinite Golden code.
- Minimum determinant $\delta_{\min} = 1/5$: this preserves the coding gain for any Q-QAM size.
- Achieves the diversity multiplexing gain frontier for 2TX-2RX antennas [10]

These particular properties of the Golden code are the key to its performance improvement over all previously proposed codes. The NVD property is especially useful for adaptive modulation schemes or whenever we need to expand the constellation to compensate for a rate loss caused by an outer code, as in TCM.

A. Uncoded Golden Code

At any time t, the received signal matrix $Y = (y_{ij}) \in \mathbb{C}^{2\times 2}$ can be written as

$$Y = \boldsymbol{H}X + Z \tag{9}$$

where $\boldsymbol{H} = (h_{ij})$ is the channel matrix, $X = (x_{ij})$ the transmitted signal matrix, and $Z = (z_{ij})$ the noise matrix. Vectorizing and separating real and imaginary parts in (9) yields

$$\boldsymbol{y} = \mathcal{H}\boldsymbol{x} + \boldsymbol{z}, \tag{10}$$

where $\boldsymbol{y}, \boldsymbol{z}, \boldsymbol{x}, \mathcal{H}$ are given in (11), (12), (13), and (14), respectively, at the bottom of the page. Lattice decoding is employed to find $\boldsymbol{x}$ such that

$$\min_{\boldsymbol{x}\in\boldsymbol{R}\mathbb{Z}^8} \|\boldsymbol{y} - \mathcal{H}\boldsymbol{x}\|^2 \tag{15}$$

$$\boldsymbol{y} = [\Re(y_{11}), \Im(y_{11}), \Re(y_{21}), \Im(y_{21}), \Re(y_{12}), \Im(y_{12}), \Re(y_{22}), \Im(y_{22})]^T \tag{11}$$

$$\boldsymbol{z} = [\Re(z_{11}), \Im(z_{11}), \Re(z_{21}), \Im(z_{21}), \Re(z_{12}), \Im(z_{12}), \Re(z_{22}), \Im(z_{22})]^T \tag{12}$$

$$\boldsymbol{x} = [\Re(x_{11}), \Im(x_{11}), \Re(x_{21}), \Im(x_{21}), \Re(x_{12}), \Im(x_{12}), \Re(x_{22}), \Im(x_{22})]^T \tag{13}$$

$$\mathcal{H} = \begin{bmatrix} \Re(h_{11}) & -\Im(h_{11}) & \Re(h_{12}) & -\Im(h_{12}) & 0 & 0 & 0 & 0 \\ \Im(h_{11}) & \Re(h_{11}) & \Im(h_{12}) & \Re(h_{12}) & 0 & 0 & 0 & 0 \\ \Re(h_{21}) & -\Im(h_{21}) & \Re(h_{22}) & -\Im(h_{22}) & 0 & 0 & 0 & 0 \\ \Im(h_{21}) & \Re(h_{21}) & \Im(h_{22}) & \Re(h_{22}) & 0 & 0 & 0 & 0 \\ 0 & 0 & 0 & 0 & \Re(h_{11}) & -\Im(h_{11}) & \Re(h_{12}) & -\Im(h_{12}) \\ 0 & 0 & 0 & 0 & \Im(h_{11}) & \Re(h_{11}) & \Im(h_{12}) & \Re(h_{12}) \\ 0 & 0 & 0 & 0 & \Re(h_{21}) & -\Im(h_{21}) & \Re(h_{22}) & -\Im(h_{22}) \\ 0 & 0 & 0 & 0 & \Im(h_{21}) & \Re(h_{21}) & \Im(h_{22}) & \Re(h_{22}) \end{bmatrix}. \tag{14}$$

Authorized licensed use limited to: University of South Australia. Downloaded on November 23, 2008 at 22:42 from IEEE Xplore. Restrictions apply.

TABLE I
THE GOLDEN CODE PARTITION CHAIN WITH CORRESPONDING LATTICES, BINARY CODES, AND MINIMUM DETERMINANTS

k	Golden subcode	Lattice	Binary code	$\Delta_{\min}$
0	$\mathcal{G}$	$\mathbb{Z}^8$	$C_0 = (8,8,1)$	$\delta_{\min}$
1	$\mathcal{G}_1$	D_4^2	$C_1 = (8,6,2)$	$2\delta_{\min}$
2	$\mathcal{G}_2$	E_8	$C_2 = (8,4,4)$	$4\delta_{\min}$
3	$\mathcal{G}_3$	L_8	$C_3 = (8,2,4)$	$8\delta_{\min}$
4	$\mathcal{G}_4 = 2\mathcal{G}$	$2\mathbb{Z}^8$	$C_4 = (8,0,\infty)$	$16\delta_{\min}$

where

$$\boldsymbol{R} = \frac{1}{\sqrt{5}} \begin{bmatrix} 1 & -\bar{\theta} & \theta & 1 & 0 & 0 & 0 & 0 \\ \bar{\theta} & 1 & -1 & \theta & 0 & 0 & 0 & 0 \\ 0 & 0 & 0 & 0 & -\theta & -1 & 1 & -\bar{\theta} \\ 0 & 0 & 0 & 0 & 1 & -\theta & \bar{\theta} & 1 \\ 0 & 0 & 0 & 0 & 1 & -\bar{\theta} & \theta & 1 \\ 0 & 0 & 0 & 0 & \bar{\theta} & 1 & -1 & \theta \\ 1 & -\theta & \bar{\theta} & 1 & 0 & 0 & 0 & 0 \\ \theta & 1 & -1 & \bar{\theta} & 0 & 0 & 0 & 0 \end{bmatrix} \tag{16}$$

is a rotation matrix preserving the shape of the QAM information symbols a, b, c, d. For this reason, we will identify the Golden code with the rotated lattice $\boldsymbol{R}\mathbb{Z}^8 = \{\boldsymbol{x} = \boldsymbol{R}\boldsymbol{u}\}$ where

$$\boldsymbol{u} = [\Re(a), \Im(a), \Re(b), \Im(b), \Re(c), \Im(c), \Re(d), \Im(d)].^T \tag{17}$$

The lattice decoding problem can be rewritten as

$$\min_{\boldsymbol{u}\in\mathbb{Z}^8} \|\boldsymbol{y} - \mathcal{H}\boldsymbol{R}\boldsymbol{u}\|^2. \tag{18}$$

B. Golden Subcodes

Let us consider a subcode $\mathcal{G}_1$ obtained as right principal ideal of the Golden code $\mathcal{G}$ [18]. In particular, we consider the subcode $\mathcal{G}_1 = \{XB, X \in \mathcal{G}\}$, where

$$B = \begin{bmatrix} i(1-\theta) & 1-\theta \\ i\theta & i\theta \end{bmatrix}. \tag{19}$$

Since B has the determinant of $1+i$, the minimum determinant of $\mathcal{G}_1$ will be $2\delta_{\min}$.

Similarly, we consider the subcodes $\mathcal{G}_k \subseteq \mathcal{G}$ for $k = 1, \ldots, 4$, defined as

$$\mathcal{G}_k = \{XB^k, X \in \mathcal{G}\} \tag{20}$$

which provide the minimum determinant $2^k\delta_{\min}$ (see Table I).

In the previous section, we have seen how the Golden codewords correspond to the rotated $\mathbb{Z}^8$ lattice points. Neglecting the rotation matrix $\boldsymbol{R}$, we can define an isomorphism between $\mathcal{G}$ and $\mathbb{Z}^8$. All the subcodes of $\mathcal{G}$ correspond to particular sublattices of $\mathbb{Z}^8$ which are listed in Table I. In particular, it can be shown that the codewords of $\mathcal{G}_2$, when vectorized, correspond to Gosset lattice points E_8 (see Appendix I). Similarly, we find that $\mathcal{G}_1$ corresponds to the lattice D_4^2 (the direct sum of two four-dimensional Shäfli lattices) and $\mathcal{G}_3$ corresponds to an eight-dimensional lattice that is denoted by L_8. Finally, since $B^4 = 2\boldsymbol{I}_2$, we get the scaled Golden code $2\mathcal{G}$ corresponding to $2\mathbb{Z}^8$.

Appendix II provides a simple overview of two basic techniques, which will play a key role in rest of the paper: *Construction A* for lattices [21] and *lattice set partitioning* by coset codes [15], [16].

As described in Appendix II, since the subcodes of $\mathcal{G}$ are nested, the corresponding lattices form the following *lattice partition chain*:

$$\mathbb{Z}^8 \supset D_4^2 \supset E_8 \supset L_8 \supset 2\mathbb{Z}^8. \tag{21}$$

Any two consecutive lattices $\Lambda_k \supset \Lambda_{k+1}$ in this chain form a four-way partition, i.e., the quotient group Λ_k/Λ_{k+1} has order 4. Let $[\Lambda_k/\Lambda_{k+1}]$ denote the set of coset leaders of the quotient group Λ_k/Λ_{k+1}.

The lattices in the partition chain can be obtained by Construction A, using the nested sequence of linear binary codes C_k listed in Table I, where C_0 is the universe code, C_2 is the extended Hamming code or Reed–Muller code RM$(1,3)$, C_3 is a subcode of C_2, C_1 is the dual of C_3, and C_4 is the empty code with only the all-zero codeword [23]. The generator matrix G_k of the code C_k are given by

$$G_1 = \begin{bmatrix} 1 & 0 & 0 & 1 & 0 & 0 & 0 & 0 \\ 0 & 1 & 0 & 1 & 0 & 0 & 0 & 0 \\ 0 & 0 & 1 & 1 & 0 & 0 & 0 & 0 \\ 0 & 0 & 0 & 0 & 1 & 0 & 0 & 1 \\ 0 & 0 & 0 & 0 & 0 & 1 & 0 & 1 \\ 0 & 0 & 0 & 0 & 0 & 0 & 1 & 1 \end{bmatrix}$$

$$G_2 = \begin{bmatrix} 0 & 1 & 0 & 1 & 0 & 1 & 0 & 1 \\ 0 & 0 & 1 & 1 & 0 & 0 & 1 & 1 \\ 0 & 0 & 0 & 0 & 1 & 1 & 1 & 1 \\ 1 & 1 & 1 & 1 & 1 & 1 & 1 & 1 \end{bmatrix}$$

$$G_3 = \begin{bmatrix} 0 & 0 & 0 & 0 & 1 & 1 & 1 & 1 \\ 1 & 1 & 1 & 1 & 1 & 1 & 1 & 1 \end{bmatrix}.$$

Looking at G_1 we can see that C_1 is the direct sum of two parity-check codes $(4,3,2)$, this proves why it yields the lattice D_4^2 by using Construction A. Similarly, since C_3 is the direct sum of two repetition codes $(4,1,4)$, we can get some insight about the structure of the lattice L_8.

Following the track of [14]–[16], we consider a partition tree of the Golden code of depth ℓ. From a nested subcode sequence $\mathcal{G} \supseteq \mathcal{G}_{\ell_0} \supset \mathcal{G}_{\ell_0+1} \supset \cdots \supset \mathcal{G}_{\ell_0+\ell}$, we have the corresponding lattice partition chain $\mathbb{Z}^8 \supseteq \Lambda_{\ell_0} \supset \Lambda_{\ell_0+1} \supset \cdots \supset \Lambda_{\ell_0+\ell}$, where

$$\begin{aligned} \Lambda_{\ell_0} &= \Lambda_{\ell_0+1} + [\Lambda_{\ell_0}/\Lambda_{\ell_0+1}] = \cdots \\ &= \Lambda_{\ell_0+\ell} + [\Lambda_{\ell_0}/\Lambda_{\ell_0+1}] + \cdots + [\Lambda_{\ell_0+\ell-1}/\Lambda_{\ell_0+\ell}] \\ &= \Lambda_{\ell_0+\ell} + [C_{\ell_0}/C_{\ell_0+1}] + \cdots + [C_{\ell_0+\ell-1}/C_{\ell_0+\ell}]. \end{aligned}$$

This results in four way *partition tree* of depth ℓ. Fig. 1 shows an example for $\ell = 2$.

The coset leaders in $[C_k/C_{k+1}]$ form a group of order 4 isomorphic to the group $\mathbb{Z}/2\mathbb{Z} \times \mathbb{Z}/2\mathbb{Z}$, which is generated by two binary generating vectors $\boldsymbol{h}_1$ and $\boldsymbol{h}_2$, i.e.,

$$[C_k/C_{k+1}] = \{b_1\boldsymbol{h}_1 + b_2\boldsymbol{h}_2 \,|\, b_1, b_2 \in \mathrm{GF}(2)\}.$$

Authorized licensed use limited to: University of South Australia. Downloaded on November 23, 2008 at 22:42 from IEEE Xplore. Restrictions apply.

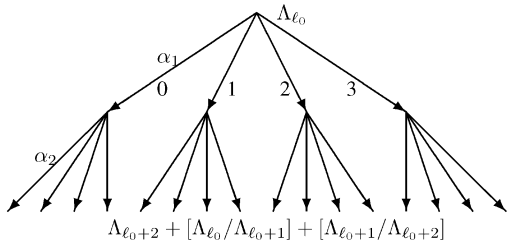


Fig. 1. Two-level ($\ell = 2$) partition tree of Λ_{ℓ_0} into 16 cosets of Λ_{ℓ_0+2}.

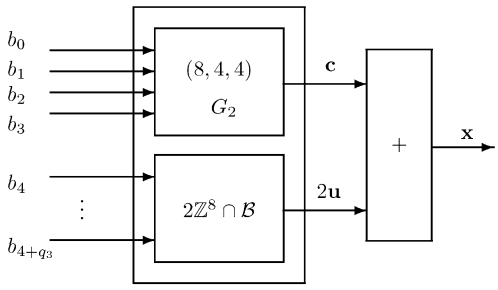


Fig. 2. The E_8 encoder structure resulting in a $\mathcal{B}$ shaped finite constellation.

If we consider all the lattices in (21) and the corresponding sequence of nested codes C_k, we have the following quotient codes with their respective generators:

$$[C_0/C_1]: \begin{cases} \boldsymbol{h}_1^{(0)} = (0,0,0,0,0,0,0,1) \\ \boldsymbol{h}_2^{(0)} = (0,0,0,1,0,0,0,0) \end{cases} \quad (22)$$

$$[C_1/C_2]: \begin{cases} \boldsymbol{h}_1^{(1)} = (0,0,0,0,0,1,0,1) \\ \boldsymbol{h}_2^{(1)} = (0,0,0,0,0,0,1,1) \end{cases}$$

$$[C_2/C_3]: \begin{cases} \boldsymbol{h}_1^{(2)} = (0,1,0,1,0,1,0,1) \\ \boldsymbol{h}_2^{(2)} = (0,0,1,1,0,0,1,1) \end{cases}$$

$$[C_3/C_4]: \begin{cases} \boldsymbol{h}_1^{(3)} = (0,0,0,0,1,1,1,1) \\ \boldsymbol{h}_2^{(3)} = (1,1,1,1,1,1,1,1). \end{cases}$$

Note that in order to generate any quotient code $[C_{\ell_0}/C_{\ell_0+\ell}]$, we stack the above vectors in the generator matrix $H(\ell_0, \ell_0+\ell)$ defined as

$$H(\ell_0, \ell_0+\ell) = \begin{pmatrix} \boldsymbol{h}_1^{(\ell_0)} \\ \boldsymbol{h}_2^{(\ell_0)} \\ \vdots \\ \boldsymbol{h}_1^{(\ell_0+\ell-1)} \\ \boldsymbol{h}_2^{(\ell_0+\ell-1)} \end{pmatrix} \quad (23)$$

so we can write

$$[C_{\ell_0}/C_{\ell_0+\ell}] = \{(b_0, b_1, \ldots, b_{2\ell_0+2\ell-2}, b_{2\ell_0+2\ell-1}) \times H(\ell_0, \ell_0+\ell) \,|\, b_k \in \text{GF}(2)\}. \quad (24)$$

For example, to generate $[C_0/C_2]$ we use the four generators to get the 16 coset leaders as

$$[C_0/C_2] = \{(b_0, b_1, b_2, b_3)H(0,2) \,|\, b_k \in \text{GF}(2)\} \quad (25)$$

where

$$H(0,2) = \begin{pmatrix} \boldsymbol{h}_1^{(0)} \\ \boldsymbol{h}_2^{(0)} \\ \boldsymbol{h}_1^{(1)} \\ \boldsymbol{h}_2^{(1)} \end{pmatrix}.$$

Note that since the $C_2 = (8,4,4)$ code is self-dual, i.e., $C_2 = C_2^{\perp}$ [23], we have

$$H(2,4) = \begin{pmatrix} \boldsymbol{h}_1^{(2)} \\ \boldsymbol{h}_2^{(2)} \\ \boldsymbol{h}_1^{(3)} \\ \boldsymbol{h}_2^{(3)} \end{pmatrix} = G_2.$$

C. Encoding and Decoding the Golden Subcodes

In this subsection, we first show how to carve a cubic shaped finite constellation from the infinite lattices corresponding to the Golden subcodes. Construction A (Appendix II) is the tool that also simplifies bit labeling for such a finite constellation. We then discuss the relation between rate and average energy required to transmit the constellation points. Finally, we analyze the decoding of the finite constellation.

We consider the sublattice $\Lambda_k \subseteq \mathbb{Z}^8$ at level k in the partition chain and the eight-dimensional bounding region $\mathcal{B} = \mathcal{B}_{\text{QAM}}^4$, the four-fold Cartesian product of the bounding region of the Q-QAM symbols. For example, using square QAM constellations, we have an eight-dimensional hypercube as bounding region.

Using Construction A, a constellation point $\boldsymbol{x} \in \Lambda_k \cap \mathcal{B}$ can be written as

$$\boldsymbol{x} = 2\boldsymbol{u} + \boldsymbol{c} \quad (26)$$

where $\boldsymbol{u} = (u_0, \ldots, u_7)$ is a eight-dimensional vector with integer components and $\boldsymbol{c} = (c_0, \ldots, c_7)$ is a binary codeword of the corresponding code C_k. With an abuse of notation, we have lifted the binary components $c_i \in \text{GF}(2)$ to integers.

Each pair of components $(2u_{2i}, 2u_{2i+1})$ is in $\mathcal{B}_{\text{QAM}}, i = 0,1,2,3$. Note that there are only $Q/4 = 2^{\eta-2}$ distinct points from the Q-QAM that correspond to pairs of components $(2u_{2i}, 2u_{2i+1}) \in \mathcal{B}_{\text{QAM}}$. Since the components c_i are either 0or 1, we are guaranteed that $(x_{2i}, x_{2i+1}) \in \mathcal{B}_{\text{QAM}}$ and $\boldsymbol{x} \in \mathcal{B}$.

We are now able to define the bit labels for the finite constellation as follows. We use $q_2 = 8 - 2k$ bits to label the 2^{q_2} codewords of C_k, through the generator matrix G_k, and $q_3 = 4(\eta - 2)$ bits to label the point $2\boldsymbol{u} \in \mathcal{B}$.

As an example, the E_8 encoder structure is shown in Fig. 2. Assuming 16-QAM symbols ($\eta = 4$), we use $q_3 = 8$ bits to label the $2\mathbb{Z}^8 \cap \mathcal{B}$ points and $q_2 = 4$ bits to select one of the codewords of C_2 as

$$\boldsymbol{c} = (b_1, b_2, b_3, b_4)G_2. \quad (27)$$

Note that there are 16 possible codewords of C_2.

We observe that the constellation $\Lambda_k \cap \mathcal{B}$ requires higher energy to transmit the same number of bits as the *uncoded Golden code constellation* $\mathbb{Z}^8 \cap \mathcal{B}'$, since $\mathcal{B}' \subset \mathcal{B}$. In particular, we have that $\text{vol}(\mathcal{B}')/\text{vol}(\mathcal{B}) = N_c$ the index of the sublattice Λ_k in $2\mathbb{Z}^8$.

For example, encoding 12 bits with E_8 requires the average energy of the 16-QAM ($E_{s,1} = 2.5$), while encoding the same number of bits with the uncoded Golden code only requires the average energy of an 8-QAM ($E_{s,2} = 1.5$). Similarly, using 128-QAM ($E_{s,1} = 20.5$) we encode 24 bits with the E_8 lattice constellation, while with an uncoded Golden code constellation we can use 64-QAM with half the energy requirements ($E_{s,2} = 10.5$).

Authorized licensed use limited to: University of South Australia. Downloaded on November 23, 2008 at 22:42 from IEEE Xplore. Restrictions apply.

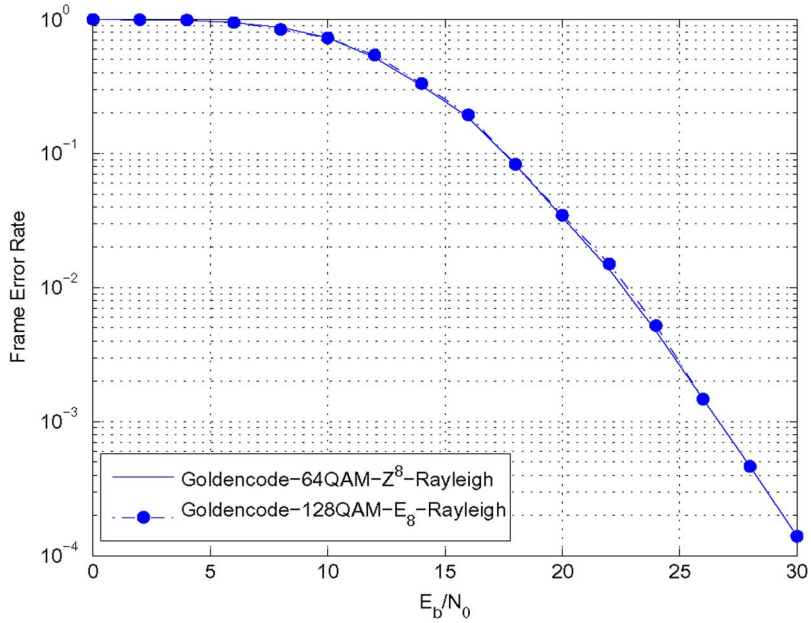


Fig. 3. Performance of $\mathbb{Z}^8$ Golden code with 64-QAM and E_8 Golden subcode with 128-QAM (12 bpcu).

Let us consider the decoding problem for the $\Lambda_k \cap \mathcal{B}$ finite constellation. Sphere decoding of finite constellations requires high additional complexity to handle the boundary control problem, when the constellation does not have a cubic shape [11]. In order to avoid this problem, we adopt the following strategy.

Given the received point $\boldsymbol{y}$, the lattice decoder first minimizes the $N_c = |\Lambda_k/2\mathbb{Z}^8|$ squared Euclidean distances in each coset

$$d_j^2 = \min_{\boldsymbol{u}^{(j)} \in \mathbb{Z}^8} \left\| \tilde{\boldsymbol{y}}^{(j)} - 2\mathcal{H}\boldsymbol{R}\boldsymbol{u}^{(j)} \right\|^2, \qquad j = 1, \ldots, N_c \quad (28)$$

where $\tilde{\boldsymbol{y}}^{(j)} = \boldsymbol{y} - \mathcal{H}\boldsymbol{R}\boldsymbol{c}^{(j)}, j = 1, \ldots, N_c$, then makes the final decision as

$$\hat{\boldsymbol{u}} = \arg \min_j \left(d_j^2 \right). \quad (29)$$

Even if we perform N_c sphere decoding operations, this strategy is rather efficient, since each decoder is working on $2\mathbb{Z}^8$ and visits on average an extremely low number of lattice points during the search. In fact, this is equivalent to working on the lattice $\mathbb{Z}^8$ at a much higher SNR.

D. Performance of the Golden Subcodes

In order to compensate for the rate loss of any subcode, a constellation expansion is required, as noted in the previous section. For large QAM constellations, it can be seen that energy increases approximately by a factor of $\sqrt{2}$ (1.5 dB) from one partition level to the next. Since the minimum determinant doubles at each partition level, we conclude that the asymptotic coding gain (6) is 1 (0 dB). However, for small constellations, the energy does not double and some gain still appears. To illustrate the observations, we show the performance of $\mathcal{G}$ and $\mathcal{G}_2$ in Figs. 3 and 4, corresponding to different spectral efficiencies. In Fig. 3, we show the performance of $\mathcal{G}$ with 64-QAM symbols ($4 \times 6 = 24$ bits per codeword) and $\mathcal{G}_2$ with 128-QAM symbols ($4 \times (7-2) + 4 = 24$ bits per codeword), corresponding to a spectral efficiency of 12 bpcu. We can see that both codes have approximately the same codeword error rate (CER). This agrees with the expected asymptotic coding gain

$$\gamma_{as} = \frac{\sqrt{4\delta_{\min}}/20.5}{\sqrt{\delta_{\min}}/10.5} = 1.02 \rightarrow 0.1 \text{ dB}.$$

Fig. 4 compares the performance of the $\mathcal{G}$ with 8-QAM symbols ($4 \times 3 = 12$ bits per codeword) and $\mathcal{G}_2$ with 16-QAM symbols ($4 \times (4-2) + 4 = 12$ bits per codeword), corresponding to the spectral efficiency of 6 bpcu. We can see that the $\mathcal{G}_2$ outperforms $\mathcal{G}$ by 0.7 dB at CER of 10^{-3}, in line with the expected asymptotic coding gain

$$\gamma_{as} = \frac{\sqrt{4\delta_{\min}}/2.5}{\sqrt{\delta_{\min}}/1.5} = 1.2 \rightarrow 0.8 \text{ dB}.$$

This small gap is essentially due to the higher energy of the 8-QAM,[1] for which $E_{s,2} = 1.5 > 2.5/\sqrt{2}$.

It is interesting to note that the E_8 constellation is the densest sphere packing in dimension 8. This implies that $\mathcal{G}_2$ maximizes

$$\min_{X \in \mathcal{G}_2, X \neq 0} \mathrm{Tr}\left(XX^{\dagger}\right) = \min_{X \in \mathcal{G}_2, X \neq 0} \|X\|_F^2$$

among all subcodes of the Golden code. Code design based on this parameter is known as a trace or Euclidean distance design criterion [19, Sec. 10.9.3]. Our result shows how this design criterion becomes irrelevant even at low SNR, when using the Golden code as a starting point.

IV. Trellis Coded Modulation

In this section, we show how a trellis code can be used as an outer code encoding across the Golden code inner symbols $X_t, t = 1, \ldots, L$. We analyze the systematic design problem of this concatenated scheme by using Ungerboeck style set partitioning rules for coset codes [14]–[16]. The design criterion

[1]This is the Cartesian product of a 4-PAM and 2-PAM constellation.

Authorized licensed use limited to: University of South Australia. Downloaded on November 23, 2008 at 22:42 from IEEE Xplore. Restrictions apply.

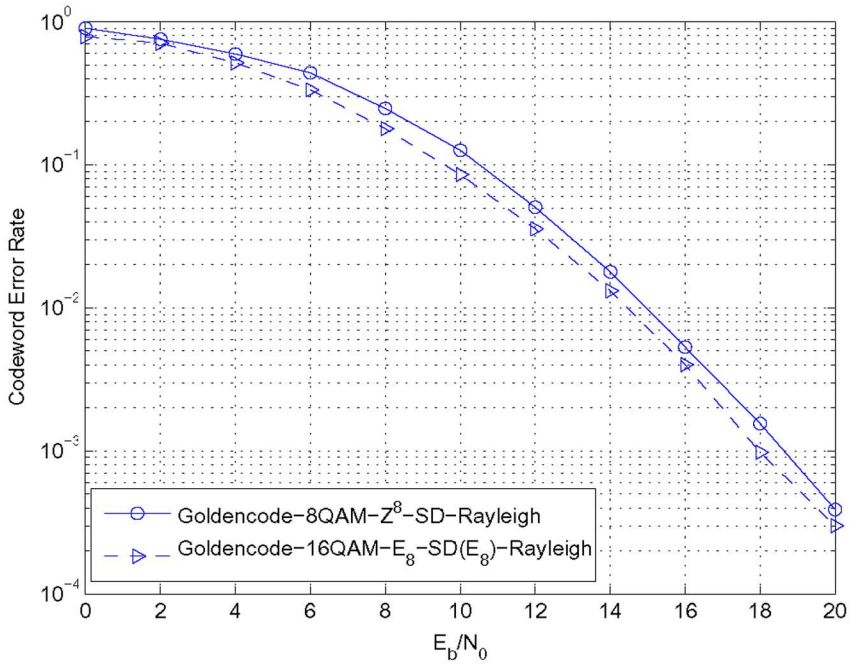


Fig. 4. Performance of $\mathbb{Z}^8$ Golden code with 8-QAM and E_8 Golden subcode with 16-QAM (6 bpcu).

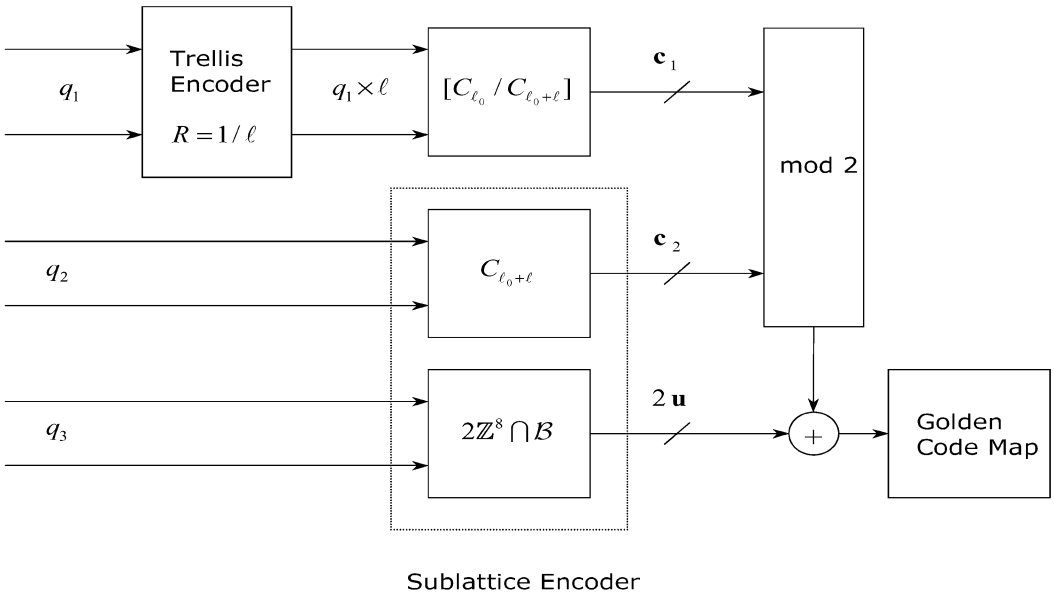


Fig. 5. General encoder structure of the concatenated scheme.

for the trellis code is developed in order to maximize $\Delta'_{\min}$, since this results in the maximum lower bound on the asymptotic coding gain of the GST-TCM over the uncoded system

$$\gamma_{as} \geq \frac{\sqrt{\Delta'_{\min}}/E_{s,1}}{\sqrt{\delta_{\min}}/E_{s,2}} = \gamma'_{as}. \tag{30}$$

We note that the asymptotic coding gain gives only a rough estimate of the actual coding gain. Nevertheless, it is currently the only means to obtain a tractable design rule for space–time TCM schemes [1]. We then show several examples of the above schemes with different rates and decoding complexity. We compare the performance of such schemes with the uncoded Golden code case.

A. Design Criteria for GST-TCM

Encoder Structure: In a standard TCM encoder the trellis encoder output is used to label the signal subset, while the uncoded bits select the signals within the subset and yield the so-called parallel transitions in the trellis [19]. Fig. 5 shows the encoder structure of the proposed concatenated scheme. The input bits feed two encoders, an upper *trellis encoder* and a lower *sublattice encoder*. The output of the trellis encoder is used to select the coset, while the sublattice encoder will select the point within the coset. The trellis will have parallel transitions on each branch corresponding to the constellation points within the same coset.

Authorized licensed use limited to: University of South Australia. Downloaded on November 23, 2008 at 22:42 from IEEE Xplore. Restrictions apply.

We consider two lattices Λ_{ℓ_0} and $\Lambda_{\ell_0+\ell}$ from the lattice partition chain in Table I, such that $\Lambda_{\ell_0+\ell}$ is a proper sublattice of the lattice Λ_{ℓ_0}, where ℓ denotes the *relative partition level* of $\Lambda_{\ell_0+\ell}$ with respect to Λ_{ℓ_0}. Let ℓ_0 denote the *absolute partition level* of the lattice Λ_{ℓ_0}. For example, with $\ell_0 = 0, \ell = 2$, we have $\Lambda_{\ell_0} = \mathbb{Z}^8$ and $\Lambda_{\ell_0+\ell} = E_8$, with $\ell_0 = 2, \ell = 2$, we have $\Lambda_{\ell_0} = E_8$ and $\Lambda_{\ell_0+\ell} = 2\mathbb{Z}^8$.

The quotient group $\Lambda_{\ell_0}/\Lambda_{\ell_0+\ell}$ has order

$$N_c = |\Lambda_{\ell_0}/\Lambda_{\ell_0+\ell}| = 4^{\ell} \tag{31}$$

which corresponds to the total number of cosets of the sublattice $\Lambda_{\ell_0+\ell}$ in the lattice Λ_{ℓ_0}.

Let us consider a trellis encoder operating on q_1 information bits. Given the relative partition depth ℓ, we need to select $N_c = 2^{2\ell}$ distinct cosets. If we consider a trellis code with rate $R_c = 1/\ell$, the trellis encoder must output

$$n_c = q_1/R_c = 2\ell = \log_2(N_c) \quad \text{bits}$$

hence we can input $q_1 = 2$ bits. Since the trellis has 2^{q_1} incoming and outgoing branches from each state, this choice is made to preserve a reasonable trellis branch complexity. The previous design, proposed in [18], had a much larger branch complexity.

The n_c bits are used by the coset mapper to label the coset leader $\boldsymbol{c}_1 \in [C_{\ell_0}/C_{\ell_0+\ell}] \sim [\Lambda_{\ell_0}/\Lambda_{\ell_0+\ell}]$. The mapping is obtained by the product of the n_c-bit vector with a binary coset leader generator matrix

$$H_{c_1} = \begin{pmatrix} \boldsymbol{h}_1^{(\ell_0)} \\ \boldsymbol{h}_2^{(\ell_0)} \\ \vdots \\ \boldsymbol{h}_1^{(\ell_0+\ell-1)} \\ \boldsymbol{h}_2^{(\ell_0+\ell-1)} \end{pmatrix} \tag{32}$$

where the rows are taken from (32).

We assume that we have a total of $4q = q_1 + q_2 + q_3$ input information bits. The lower encoder is a sublattice encoder for $\Lambda_{\ell_0+\ell}$ and operates on the remaining $q_2 + q_3$ information bits. The $q_2 = 2 \times (4 - \ell - \ell_0)$ bits label the cosets of $2\mathbb{Z}^8$ in $\Lambda_{\ell_0+\ell}$ by multiplying the following binary generator matrix:

$$H_{c_2} = \begin{pmatrix} \boldsymbol{h}_1^{(\ell_0+\ell)} \\ \boldsymbol{h}_2^{(\ell_0+\ell)} \\ \vdots \\ \boldsymbol{h}_1^{(3)} \\ \boldsymbol{h}_2^{(3)} \end{pmatrix} \tag{33}$$

which generates coset leader $\boldsymbol{c}_2 \in [\Lambda_{\ell_0+\ell}/2\mathbb{Z}^8]$. We finally add both coset leaders of $\boldsymbol{c}_1$ and $\boldsymbol{c}_2$ modulo 2 to get $\boldsymbol{c}'$. The remaining $q_3 = 4q - q_1 - q_2$ bits go through $2\mathbb{Z}^8$ encoder and generate vector $2\boldsymbol{u}$ as detailed in Appendix II. Finally, $2\boldsymbol{u}$ is added to $\boldsymbol{c}'$ (lifted to have integer components) and mapped to the Golden codeword X_t.

We now focus on the structure of the trellis code to be used. We consider linear convolutional encoders over the quaternary alphabet $\mathbb{Z}_4 = \{0, 1, 2, 3\}$ with $\bmod 4$ operations. We assume

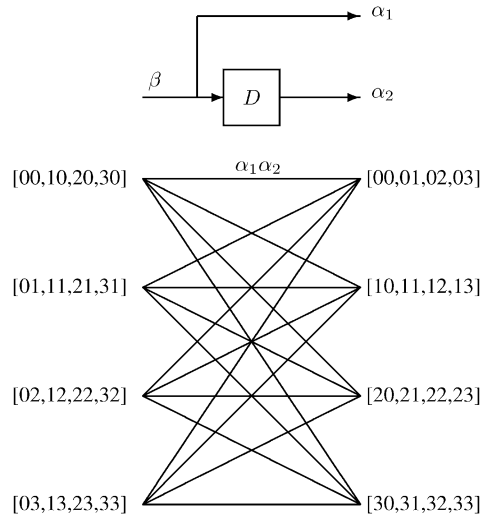


Fig. 6. The four-state encoder with $g_1(D) = 1$ and $g_2(D) = D$ and corresponding trellis diagram. Labels on the left are outgoing from each state clockwise, labels on the right are incoming counterclockwise.

the natural mapping between pairs of bits and $\mathbb{Z}_4$ symbols, i.e., $0 \to 00, 1 \to 01, 2 \to 10, 3 \to 11$. Let $\beta \in \mathbb{Z}_4$ denote the input symbol and $\alpha_1, \ldots, \alpha_\ell \in \mathbb{Z}_4$ denote the ℓ output symbols generated by the generator polynomials $g_1(D), \ldots g_\ell(D)$ over $\mathbb{Z}_4$.

For example, Fig. 6 shows a four-state encoder with rate $R_c = 1/2$ defined by the generator polynomials $g_1(D) = 1$ and $g_2(D) = D$. The trellis labels for outgoing and incoming branches listed from top to bottom. Fig. 1 shows how the $N_c = 16$ cosets can be addressed through a partition tree of depth 2.

Labeling: Let us first consider the conventional design of the trellis labeling in a TCM scheme. We then show how this can be directly transferred to GST-TCM. The conventional TCM design criteria attempt to increase the minimum Euclidean distance $d_{\min}$ between codewords in the following way.

1) Use subconstellations with a larger minimum Euclidean distance $d_{p,\min}$, known as *intra-coset distance*.
2) Label the parallel branches in the trellis with the points within the same subconstellation.
3) Label the trellis branches for different states so that the partitions can increase the *inter-coset distance* $d_{s,\min}$ among code sequences.

The aim of our GST-TCM design criteria is to maximize the lower bound $\Delta'_{\min}$ in (8). The additive structure of the $\Delta'_{\min}$ enables to use the same strategy that is used for the Euclidean distance in conventional TCM design. Let

$$\Delta_{\mathrm{p}} = 2^{\ell_0+\ell}\delta_{\min} \tag{34}$$

denote the minimum determinant on the trellis parallel transitions corresponding to the Golden code partition $\Lambda_{\ell_0+\ell}$ of absolute level $\ell_0 + \ell$. Let

$$\Delta_{\mathrm{s}} = \min_{\boldsymbol{X} \neq \boldsymbol{0}_{2\times 2L}} \sum_{t=t_o}^{t_o+L'-1} \det(X_t X_t^{\dagger}) \tag{35}$$

denote the minimum determinant on the shortest simple error event, where L' is the length of the shortest simple error event diverging from the zero state at t_o and merging to the zero state

Authorized licensed use limited to: University of South Australia. Downloaded on November 23, 2008 at 22:42 from IEEE Xplore. Restrictions apply.

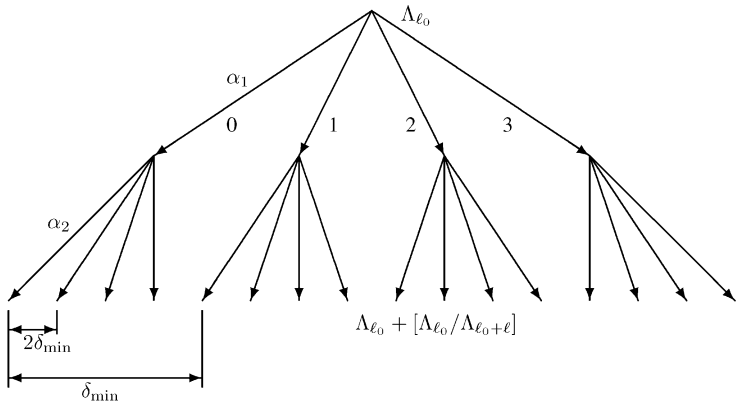


Fig. 7. Inter coset distances for a two-level partition tree.

TABLE II
SUMMARY OF THE PARAMETERS OF GST-TCM EXAMPLES

Ex.	Λ_{ℓ_0}	$\Lambda_{\ell_0+\ell}$	ℓ_0	ℓ	q_1	q_2	q_3	bpcu	Q	states	$g_1(D),\ldots,g_\ell(D)$	γ'_{as} ($\Delta_{\rm p}$)	γ'_{as} ($\Delta_{\rm s}$)	gain @ 10^{-3}
1	E_8	$2\mathbb{Z}^8$	2	2	2	0	8	5	16	4	$(1, D)$	2.0	1.4	2.2
										16	$(D, 1+D^2)$	2.0	2.5	2.5
2	$\mathbb{Z}^8$	E_8	0	2	2	4	8	7	16	4	$(1, D)$	2.0	1.4	3.0
										16	$(D, 1+D^2)$	2.0	2.5	3.3
3	$\mathbb{Z}^8$	L_8	0	3	2	2	8	6	16	16	$(D, D^2, 1+D^2)$	2.3	2.0	4.2
										64	$(D, D^2, 1+D^3)$	2.3	3.0	4.3
4	$\mathbb{Z}^8$	L_8	0	3	2	2	16	10	64	16	$(D, D^2, 1+D^2)$	1.3	1.0	1.5
										64	$(D, D^2, 1+D^3)$	1.3	2.0	1.5

at $t_i = t_o + L'$. We can increase $\Delta_{\rm s}$ in (35) either by increasing L' or by increasing the $\det(X_t X_t^\dagger)$ terms. Fig. 7 shows the possible inter coset distances contributing to (35).

Note that once L' is fixed, Ungerboeck's design rules focus on the first and last term only. The lower bound $\Delta'_{\min}$ in (8) is determined either by the parallel transition error events or by the shortest simple error events in the trellis, i.e.,

$$\begin{aligned}\Delta'_{\min} &= \min\{\Delta_{\rm p}, \Delta_{\rm s}\} \\ &\geq \min\left\{\Delta_{\rm p}, \min_{X_{t_o}} \det(X_{t_o} X_{t_o}^\dagger) + \min_{X_{t_i}} \det(X_{t_i} X_{t_i}^\dagger)\right\}. \end{aligned} \tag{36}$$

The corresponding coding gain will be

$$\gamma'_{as} = \min\{\gamma'_{as}(\Delta_{\rm p}), \gamma'_{as}(\Delta_{\rm s})\}. \tag{37}$$

Therefore, we can state the following.

Design Criterion: *We focus on $\Delta'_{\min}$. The incoming and outgoing branches for each state should belong to different cosets that have the common father node as deep as possible in the partition tree. This guarantees that simple error events in the trellis give the largest contribution to $\Delta'_{\min}$.*

In order to fully satisfy the above criterion for a given relative partition level ℓ, the minimum number of trellis states should be $N_c = 2^{2\ell}$. In order to reduce complexity we will also consider trellis codes with fewer states. We will see in the following that the performance loss of these suboptimal codes (in terms of the above design rule) is marginal since $\Delta_{\rm p}$ is dominating in (36). Nevertheless, the optimization of $\Delta_{\rm s}$ yields a performance enhancement. In fact, maximizing $\Delta_{\rm s}$ has the effect of minimizing another relevant PWEP term.

Decoding: Let us analyze the decoding complexity. The decoder is structured as a typical TCM decoder, i.e., a Viterbi algorithm using a branch metric computer. The branch metric computer should output the distance of the received symbol from all the cosets of $\Lambda_{\ell_0+\ell}$ in Λ_{ℓ_0}. The decoding complexity depends on two parameters

- N_c the total number of distinct parallel branch metrics,
- the number of states in the trellis.

We observe that the branch metric computer can be realized either as a traditional sphere decoder for each branch or as single list sphere decoder which can keep track of all the cosets at once.

B. Code Design Examples for TCM

In this subsection, we give four examples of GST-TCM with different numbers of states using different partitions $\Lambda_{\ell_0}/\Lambda_{\ell_0+\ell}$. We assume a frame length $L = 130$ in all examples. All related parameters are summarized in Table II.

The trellis code generator polynomials have been selected by an exhaustive search among all polynomials of degree less than four with quaternary coefficients. The selection was made in

Authorized licensed use limited to: University of South Australia. Downloaded on November 23, 2008 at 22:42 from IEEE Xplore. Restrictions apply.

order to satisfy the design criterion (when possible) and to maximize Δ_s.

We first describe the uncoded Golden code schemes, which are used as reference systems for performance comparison. In the standard uncoded Golden code, four Q-QAM information symbols are sent for each codeword (2), for a total of $4q$ information bits, where $q = \log_2(Q)$. When q is not integer, we have to consider different size QAM symbols within the same Golden codeword, as shown in the following examples.

- **5 bpcu**—A total of 10 bits must be sent in a Golden codeword: the symbols a and c are in a 4-QAM (2 bits), while the symbols b and d are in a 8-QAM (3 bits). This guarantees that the same average energy is transmitted from both antennas. In this case, we have $E_{s,2} = (0.5 + 1.5)/2 = 1$ and $q = 2.5$ bits.
- **6 bpcu**—A total of 12 bits must be sent in a Golden codeword: the symbols a, b, c, d are in a 8-QAM (3 bits). In this case, we have $E_{s,2} = 1.5$ and $q = 3$ bits.
- **7 bpcu**—A total of 14 bits must be sent in a Golden codeword: the symbols a and c are in a 8-QAM (3 bits), while the symbols b and d are in a 16-QAM (4 bits). This guarantees that the same average energy is transmitted from both antennas. In this case, we have $E_{s,2} = (1.5 + 2.5)/2 = 2$ and $q = 3.5$ bits.
- **10 bpcu**—A total of 20 bits must be sent in a Golden codeword: the symbols a, b, c, d are in a 32-QAM (5 bits). In this case, we have $E_{s,2} = 5$ and $q = 5$ bits.

Example 1: We use a two level partition $E_8/2\mathbb{Z}^8$. The 4- and 16-state trellis codes using 16-QAM $(E_{s,1} = 2.5)$ gain 2.2 and 2.5 dB, respectively, over the uncoded Golden code $(E_{s,2} = 1)$ at the rate of 5 bpcu.

The two-level partition ($\ell_0 = 2$ and $\ell = 2$) has a quotient group $E_8/2\mathbb{Z}^8$ of order $N_c = 16$. The quaternary trellis encoders for 4 and 16 states with rate $R_c = 1/2$, have $q_1 = 2$ input information bits and $n_c = 4$ output bits, which label the coset leaders using the generator matrix with rows $\boldsymbol{h}_1^{(2)}, \boldsymbol{h}_2^{(2)}, \boldsymbol{h}_1^{(3)}, \boldsymbol{h}_2^{(3)}$. The trellis structures are shown in Figs. 6 and 8, respectively. The sublattice encoder has $q_2 = 0$ and $q_3 = 8$ input bits, giving a total number of input bits per information symbol $q = (q_1 + q_2 + q_3)/4 = 10/4 = 2.5$ bits.

In Fig. 6, for each trellis state, the four outgoing branches with labels α_1, α_2, corresponding to input $\beta = 0, 1, 2, 3$, are listed on the left side of the trellis. Similarly, four incoming trellis branches to each state are listed on the right side of the trellis structure. In this case, α_1 chooses the cosets from L_8 in $\Lambda = E_8$ and α_2 chooses the cosets from $\Lambda_\ell = 2\mathbb{Z}^8$ in L_8.

We can observe that the four branches merging in each state belong to four different cosets of $2\mathbb{Z}^8$ in L_8, since α_1 is constant and α_2 varies (see Fig. 10). This guarantees an increased $\Delta'_{\min}$. On the other hand, the four branches departing from each state are in the cosets of L_8 in E_8. This does not give the largest possible $\Delta'_{\min}$ since α_1 varies. Looking, for example, at the zero state, there are four outgoing branches labeled by $\alpha_1 = 0, 1, 2, 3$, and α_2 is fixed to 0, while the four incoming branches are labeled by $\alpha_1 = 0$ and $\alpha_2 = 0, 1, 2, 3$.

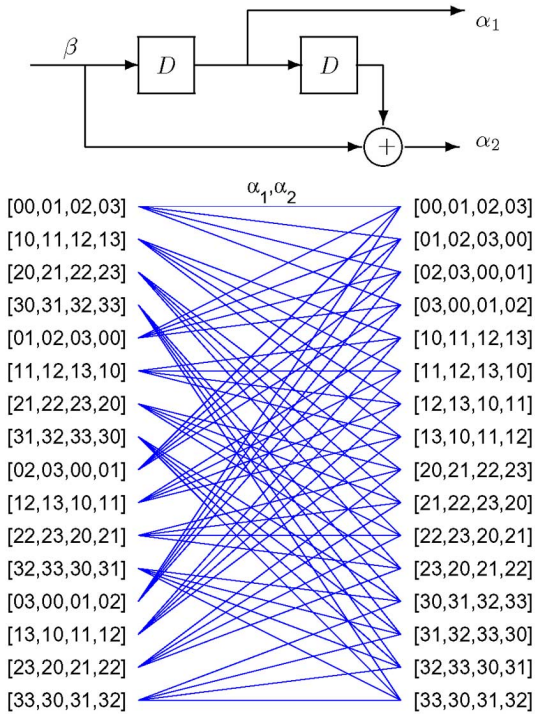


Fig. 8. The optimal 16-states trellis corresponding to the generators $g_1(D) = D$ and $g_2(D) = 1 + D^2$. Labels on the left are outgoing from each state clockwise, labels on the right are incoming counterclockwise.

This results in a suboptimal design since it cannot guarantee that the outgoing trellis paths belong to cosets that are in the deepest level $(2\mathbb{Z}^8)$ of the partition tree. We can see that the shortest simple error event has a length of $L' = 2$, corresponding to the state sequence $0 \to 1 \to 0$ and labels 10, 01. This yields the lower bound on the asymptotic coding gain

$$\gamma'_{as} = \frac{\sqrt{\min(16\delta_{\min}, 4\delta_{\min} + 8\delta_{\min})}/E_{s,1}}{\sqrt{\delta_{\min}}/E_{s,2}} \to 1.4 \text{ dB}. \quad (38)$$

The above problem suggests the use of a 16-state encoder. In Fig. 8, we can see that the shortest simple error event has length $L' = 3$ corresponding to the state sequence $0 \to 1 \to 4 \to 0$ and labels $01, 10, 01$. In general, we have that the first output label α_1 is fixed for both outgoing and incoming states. This guarantees both incoming and outgoing trellis branches from each state belong cosets with the deepest father nodes in the partition tree. This yields the lower bound on the corresponding asymptotic coding gain

$$\gamma'_{as} = \frac{\sqrt{\min(16\delta_{\min}, 8\delta_{\min} + 4\delta_{\min} + 8\delta_{\min})}/E_{s,1}}{\sqrt{\delta_{\min}}/E_{s,2}} \to 2.0 \text{ dB}. \quad (39)$$

Compared to 4-state, the 16-state GST-TCM has a higher decoding complexity. It requires 64 lattice decoding operations in each trellis section, while the 4-state GST-TCM only requires 16 lattice decoding operations. Note that each lattice decoding operation is working on $2\mathbb{Z}^8$.

Authorized licensed use limited to: University of South Australia. Downloaded on November 23, 2008 at 22:42 from IEEE Xplore. Restrictions apply.

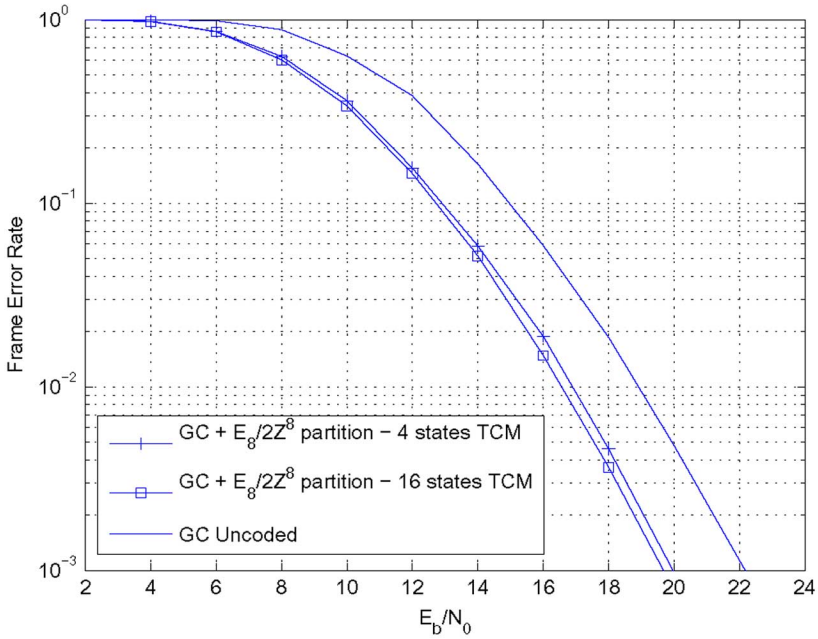


Fig. 9. Performance comparison of a 4-state trellis code using 16-QAM constellation and an uncoded transmission at the rate 5 bpcu, $\Lambda = E_8, \Lambda_\ell = 2\mathbb{Z}^8, \ell = 2$ (see Example 1).

Performance comparison of the proposed codes with the uncoded scheme with 5 bpcu is shown in Fig. 9. We can observe that a simple 4–state GST-TCM outperforms the uncoded scheme by 2.2 dB at the FER of 10^{-3}. The 16-state GST-TCM outperforms the uncoded case by 2.5 dB at the FER of 10^{-3}.

Example 2: We use a two-level partition $\mathbb{Z}^8/E_8$ ($\ell_0 = 0$ and $\ell = 2$). The 4- and 16-state trellis codes using 16-QAM $(E_{s,1} = 2.5)$ gain 3.0 and 3.3 dB, respectively, over uncoded Golden code $(E_{s,2} = 2)$ at the rate of 7 bpcu.

As in Example 1, we can see that the 4-state trellis code is suboptimal since it cannot guarantee that both the incoming and outgoing trellis paths belong to cosets that are in the deepest level (E_8) of the partition tree. In contrast, the 16-state trellis code always has a fixed label α_1 in each state. This fully satisfies the proposed design criteria. However, the 16-state code requires higher decoding complexity. Finally, we have

$$\gamma'_{as} = \frac{\sqrt{\min(4\delta_{\min}, \delta_{\min} + 2\delta_{\min})}/E_{s,1}}{\sqrt{\delta_{\min}}/E_{s,2}} \to 1.4 \text{ dB} \quad (40)$$

for the 4-state GST-TCM and

$$\gamma'_{as} = \frac{\sqrt{\min(4\delta_{\min}, 2\delta_{\min} + \delta_{\min} + 2\delta_{\min})}/E_{s,1}}{\sqrt{\delta_{\min}}/E_{s,2}} \to 2.0 \text{ dB} \quad (41)$$

for the 16-state GST-TCM.

Performance of both the proposed TCM and uncoded transmission (7 bpcu) schemes is compared in Fig. 10. It is shown that the proposed 4- and 16-state TCMs outperform the uncoded case by 3.0 and 3.3 dB at the FER of 10^{-3}.

Compared to Example 1, this GST-TCM has a higher decoding complexity. It requires $N_c = 256$ lattice decoding operations of $2\mathbb{Z}^8$ in each trellis section or 16 lattice decoders of cosets of E_8.

Example 3: We use a three-level partition $\mathbb{Z}^8/L_8$ ($\ell_0 = 0$ and $\ell = 3$). The 16- and 64-state trellis codes using 16-QAM $(E_{s,1} = 2.5)$ gain 4.2 and 4.3 dB, respectively, over an uncoded Golden code $(E_{s,2} = 1.5)$ at the rate of 6 bpcu.

In Fig. 12, for each trellis state, the four outgoing branches with labels $\alpha_1, \alpha_2, \alpha_3$, corresponding to input $\beta = 0, 1, 2, 3$, are listed on the left side of the trellis. Similarly, the four incoming trellis branches to each state are listed on the right side of the trellis structure. In such a case, α_1 chooses the cosets from D_4^2 in $\Lambda = \mathbb{Z}^8$, α_2 chooses the cosets from E_8 in D_4^2, and α_3 chooses the cosets from $\Lambda_\ell = L_8$ in E_8.

The four branches departing from each state belong to four different cosets of L_8, since α_1 and α_2 are constant, while α_3 varies. On the other hand, the four branches arriving in each state are cosets of E_8. This does not yield the largest possible $\Delta'_{\min}$, since only α_1 is fixed but α_2 varies. This results in a suboptimal design since it cannot guarantee that both incoming and outgoing trellis paths belong to cosets that are in the deepest level (L_8) of the partition tree.

We can see that the shortest simple error event has a length of $L' = 3$ corresponding to the state sequence $0 \to 1 \to 4 \to 0$ and labels $001, 100, 011$. This yields the lower bound of the corresponding asymptotic coding gain

$$\gamma'_{as} = \frac{\sqrt{\min(8\delta_{\min}, 4\delta_{\min} + \delta_{\min} + 2\delta_{\min})}/E_{s,1}}{\sqrt{\delta_{\min}}/E_{s,2}} \to 2.0 \text{ dB}. \quad (42)$$

The above problem suggests the use of a 64-state encoder. In Fig. 8, we can see that the shortest simple error event has length $L' = 4$ corresponding to the state sequence $0 \to 1 \to 4 \to 16 \to 0$ and labels $001, 100, 010, 001$. Note that now the output labels α_1, α_2 are fixed for all outgoing

Authorized licensed use limited to: University of South Australia. Downloaded on November 23, 2008 at 22:42 from IEEE Xplore. Restrictions apply.

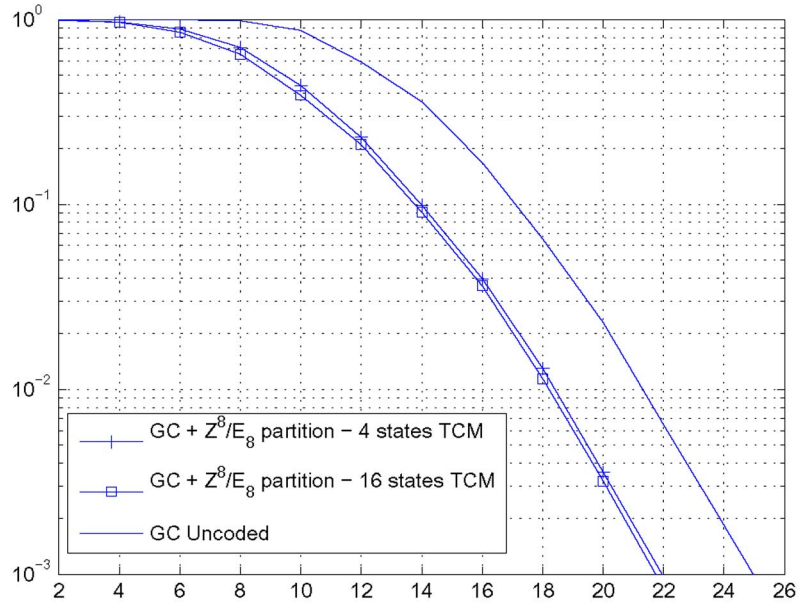


Fig. 10. Performance comparison of 4- and 16-state trellis codes using 16-QAM constellation and an uncoded transmission at the rate of 7 bpcu and $\Lambda = \mathbb{Z}^8$, $\Lambda_\ell = E_8$, $\ell = 2$ (see Example 2).

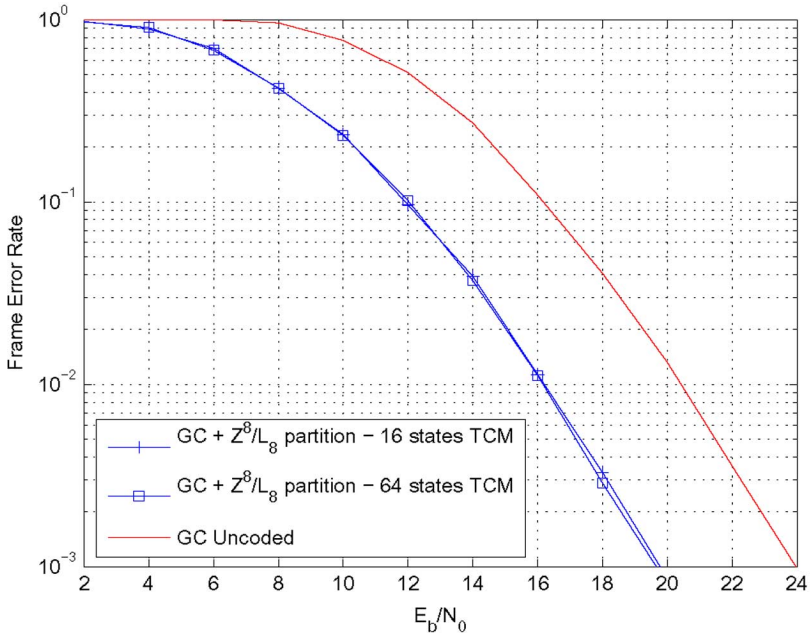


Fig. 11. Performance comparison of 16- and 64- state trellis codes using 16-QAM constellation and an uncoded transmission at the rate of 6 bpcu and $\Lambda = \mathbb{Z}^8, \Lambda_\ell = L_8, \ell = 3$ (see Example 3).

and incoming states. This guarantees that both incoming and outgoing trellis branches from each state belong to the cosets that are deepest in the partition tree. This yields the lower bound of the corresponding asymptotic coding gain

$$\gamma'_{as} = \frac{\sqrt{\min(8\delta_{\min}, 4\delta_{\min} + \delta_{\min} + 2\delta_{\min} + 4\delta_{\min})}/E_{s,1}}{\sqrt{\delta_{\min}}/E_{s,2}} \rightarrow 2.3 \text{ dB}. \quad (43)$$

Performance of the proposed codes and the uncoded scheme with 6 bpcu is compared in Fig. 11. We can observe that a 16-state GST-TCM outperforms the uncoded scheme by 4.2 dB at the FER of 10^{-3}. The 64-state GST-TCM outperforms the uncoded case by 4.3 dB at FER of 10^{-3}.

Note that in the Example with 16 states, we have the same decoding complexity as in the previous example with 16 states.

Example 4: We use the same partition as in Example 3. The 16-and 64-state trellis codes using 64-QAM $(E_{s,1} = 10.5)$ *gain 1.5 dB, in both cases, over an uncoded Golden code* $(E_{s,2} = 5)$ *at the rate of* 10.

The trellis structures are shown in Figs. 12 and 14, respectively. This yields the lower bounds of the corresponding asymptotic coding gain

$$\gamma'_{as} = \frac{\sqrt{\min(8\delta_{\min}, 4\delta_{\min} + \delta_{\min} + 2\delta_{\min})}/E_{s,1}}{\sqrt{\delta_{\min}}/E_{s,2}} \rightarrow 1.0 \text{ dB} \quad (44)$$

Authorized licensed use limited to: University of South Australia. Downloaded on November 23, 2008 at 22:42 from IEEE Xplore. Restrictions apply.

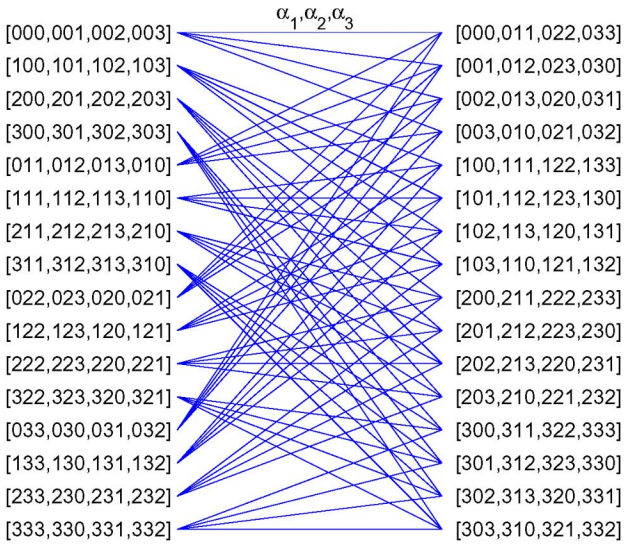


Fig. 12. The 16-states trellis corresponding to the generators $g_1(D) = D, g_2(D) = D^2$, and $g_3(D) = 1 + D^2$. Labels on the left are outgoing from each state clockwise, labels on the right are incoming counterclockwise.

for the 16-state GST-TCM and

$$\gamma'_{as} = \frac{\sqrt{\min(8\delta_{\min}, 4\delta_{\min} + \delta_{\min} + 2\delta_{\min} + 4\delta_{\min})}/E_{s,1}}{\sqrt{\delta_{\min}}/E_{s,2}} \rightarrow 1.3\ \text{dB} \tag{45}$$

for the 64-state GST-TCM.

Fig. 13 compares the performance of the above codes at the spectral efficiency of 10 bpcu with 64-QAM signal constellation for GST-TCM and 32-QAM signal constellation for uncoded case, respectively. It is shown that a 16-state GST-TCM outperforms the uncoded scheme by 1.5 dB at the FER of 10^{-3}. The 64-state code has similar performance as the 16-state code.

Remarks: For GST-TCM, we can see that the lower bound γ'_{as} on γ_{as} is only a rough approximation of the true system performance. This is due to the following reasons:

1) γ_{as} is based on the worst case pairwise error event which is not always the strongly dominant term of the full union bound in fading channels;
2) the lower bound γ'_{as} on γ_{as} can be loose due to the determinant inequality;
3) the multiplicity of the minimum determinant paths is not taken into account.

Looking at Table II, we observe that the true coding gain is better approximated by a combination of $\gamma'_{as}(\Delta_{\mathrm{p}})$ and $\gamma'_{as}(\Delta_{\mathrm{s}})$ in (37), rather than γ'_{as}.

V. Conclusion

In this paper, we presented GST-TCM, a concatenated scheme for slow-fading 2×2 MIMO systems. The inner code is the Golden code and the outer code is a trellis code. Lattice set partitioning is designed specifically to increase the minimum determinant of the Golden codewords, which label the branches of the outer trellis code. Viterbi algorithm is applied in trellis decoding, where branch metrics are computed by using a lattice sphere decoder. The general framework for GST-TCM design and optimization is based on Ungerboeck TCM design rules.

Simulation shows that 4- and 16-state GST-TCMs achieve 3 and 4.2 dB performance gains over uncoded Golden code at FER of 10^{-3} with spectral efficiencies of 7 and 6 bpcu, respectively.

Future work will explore the possibility of further code optimization, by an extensive search based on the determinant distance spectrum, which gives a more accurate approximation of the true coding gain.

Appendix I
Proof of (20)

Let us consider a subcode $\mathcal{G}_2$ of the Golden code $\mathcal{G}$ obtained by $\mathcal{G}_2 = \{XB^2, X \in \mathcal{G}\}$, where B is given in (19) and X is given as

$$X = \begin{bmatrix} \alpha(a+b\theta) & \alpha(c+d\theta) \\ i\bar{\alpha}(c+d\bar{\theta}) & \bar{\alpha}(a+b\bar{\theta}) \end{bmatrix} \tag{46}$$

where we omit the normalization factor $\frac{1}{\sqrt{5}}$ for simplicity. After manipulations, we obtain the subcode $\mathcal{G}_2$ codeword

$$\begin{bmatrix} g_{11} & g_{12} \\ g_{21} & g_{22} \end{bmatrix} = XB^2 \tag{47}$$

where $g_{11}, g_{12}, g_{21}, g_{22}$ are given by

$$\begin{aligned} g_{11} &= [-1 - i2(1+\bar{\theta})]a + (-\theta + i2\bar{\theta})b \\ &\quad + (-\theta + i)c + (-1 - \theta + i\theta)d \qquad (48) \\ g_{21} &= [-\theta - i(1+\theta)]a + (1 + i\theta)b \\ &\quad + [\theta - i2\bar{\theta}]c + [-1 - i(2 + 2\bar{\theta})]d \qquad (49) \\ g_{12} &= [-1 - \bar{\theta} + i\bar{\theta}]a + (\bar{\theta} - i)b \\ &\quad + (-2\theta - i\bar{\theta})c + (-2 - 2\theta + i)d \qquad (50) \\ g_{22} &= [-1 - i2(1+\theta)]a + (-\bar{\theta} + i2\theta)b \\ &\quad + (-1 + \theta + i)c + (-1 - \bar{\theta} + i\bar{\theta})d. \qquad (51) \end{aligned}$$

Note that $\bar{\theta} = 1 - \theta$ and $\theta^2 = \theta + 1$. Vectorizing (47) yields

$$\mathrm{vec}(XB^2) = \tilde{\boldsymbol{R}}\boldsymbol{u} \tag{52}$$

where $\mathrm{vec}(XB^2)$ is given by (53) and $\tilde{\boldsymbol{R}}, \boldsymbol{u}$ are given by (54) at the bottom of the following page. The matrix $\tilde{\boldsymbol{R}}$ can be written as

$$\tilde{\boldsymbol{R}} = \boldsymbol{R}\tilde{\boldsymbol{M}}.$$

Substituting the matrix $\boldsymbol{R}$, defined in (16), into above equation yields the lattice generator matrix

$$\tilde{\boldsymbol{M}} = \boldsymbol{R}^T\tilde{\boldsymbol{R}} = \begin{bmatrix} -2 & 1 & 1 & 0 & 0 & 0 & -1 & 0 \\ -1 & -2 & 0 & 1 & 0 & 0 & 0 & -1 \\ 1 & 0 & -1 & 1 & -1 & 0 & -1 & 0 \\ 0 & 1 & -1 & -1 & 0 & -1 & 0 & -1 \\ 0 & -1 & 0 & 1 & -1 & 1 & -1 & 0 \\ 1 & 0 & -1 & 0 & -1 & -1 & 0 & -1 \\ 0 & 1 & 0 & 0 & -1 & 0 & -2 & 1 \\ -1 & 0 & 0 & 0 & 0 & -1 & -1 & -2 \end{bmatrix}.$$

By conducting Lenstra–Lenstra–Lovász (LLL) lattice basis reduction, we found that the lattice generator matrix $\tilde{\boldsymbol{M}}$ has the

Authorized licensed use limited to: University of South Australia. Downloaded on November 23, 2008 at 22:42 from IEEE Xplore. Restrictions apply.

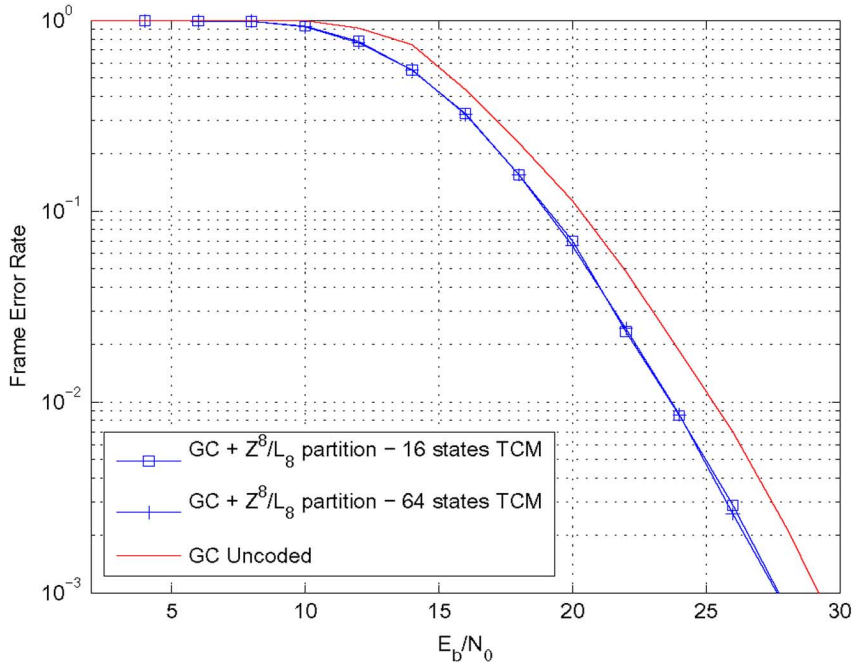


Fig. 13. Performance comparison of 16- and 64-state trellis codes using 64-QAM constellation and an uncoded transmission at the rate of 10 bpcu and $\Lambda = \mathbb{Z}^8, \Lambda_\ell = L_8, \ell = 3$ (see Example 4).

minimum squared Euclidean distance $d^2_{\min} = 4$. Since the determinant of $\tilde{\boldsymbol{M}}$ is 16, the packing density coincides with the one of E_8, which is the unique optimal sphere packing in dimension 8. Note that there exist multiple lattice generator matrices for E_8 lattices, all of which have the same properties as above [21]. Therefore, we conclude that the subcode $\mathcal{G}_2$ of the Golden code $\mathcal{G}$, when vectorized, corresponds to the E_8 lattice points. A similar approach can be used for the other lattices in the partition. □

Appendix II
Construction A and Set Partitioning

In this appendix, we review the basic principles of *Construction A* and *lattice set partitioning* by coset codes following a simple example based on the lattice $\mathbb{Z}^2$. The general theory underlying these techniques is described in detail in [21], [15], [16]. We assume that the reader is familiar with the basic facts of group theory, in particular, we will use the notions of group, subgroup, quotient group, and group isomorphism [20].

Construction A establishes a correspondence between an integer lattice and a linear binary code [21]. In particular, given an integer lattice Λ we obtain all the codewords of a linear binary code C by taking all components of the lattice points $\bmod 2$, we write

$$C = \Lambda \bmod 2. \tag{55}$$

On the other hand, given a linear binary code $C = (n, k, d)$ with codewords $\boldsymbol{c}_i$ we can write

$$\Lambda = 2\mathbb{Z}^n + C = \bigcup_{\boldsymbol{c}_i \in C} (2\mathbb{Z}^n + \boldsymbol{c}_i). \tag{56}$$

This construction provides also a simple relation between the minimum Hamming distance d of the code and the minimum Euclidean distance between any two lattice points. For this reason, it can be used to design dense sphere packing lattices

$$\operatorname{vec}(XB^2) = [\Re(g_{11}), \Im(g_{11}), \Re(g_{21}), \Im(g_{21}), \Re(g_{12}), \Im(g_{12}), \Re(g_{22}), \Im(g_{22})]^T \tag{53}$$

$$\tilde{\boldsymbol{R}} = \begin{bmatrix} -1 & 2(1+\bar{\theta}) & -\theta & -2\bar{\theta} & -\theta & -1 & -1-\theta & -\theta \\ -2(1+\bar{\theta}) & -1 & 2\bar{\theta} & -\theta & 1 & -\theta & \theta & -1-\theta \\ -\theta & 1+\theta & 1 & -\theta & \theta & 2\bar{\theta} & -1 & 2+2\bar{\theta} \\ -1-\theta & -\theta & \theta & 1 & -2\bar{\theta} & \theta & -2-2\bar{\theta} & -1 \\ -1-\bar{\theta} & -\bar{\theta} & \bar{\theta} & 1 & -2\theta & \bar{\theta} & -2-2\theta & -1 \\ \bar{\theta} & -1-\bar{\theta} & -1 & \bar{\theta} & -\bar{\theta} & -2\theta & 1 & -2-2\theta \\ -1 & 2(1+\theta) & -\bar{\theta} & -2\theta & -1+\theta & -1 & -1-\bar{\theta} & -\bar{\theta} \\ -2(1+\theta) & -1 & 2\theta & -\bar{\theta} & 1 & -1+\theta & \bar{\theta} & -1-\bar{\theta} \end{bmatrix} \tag{54}$$

and

$$\boldsymbol{u} = [\Re(a), \Im(a), \Re(b), \Im(b), \Re(c), \Im(c), \Re(d), \Im(d)]^T.$$

Authorized licensed use limited to: University of South Australia. Downloaded on November 23, 2008 at 22:42 from IEEE Xplore. Restrictions apply.

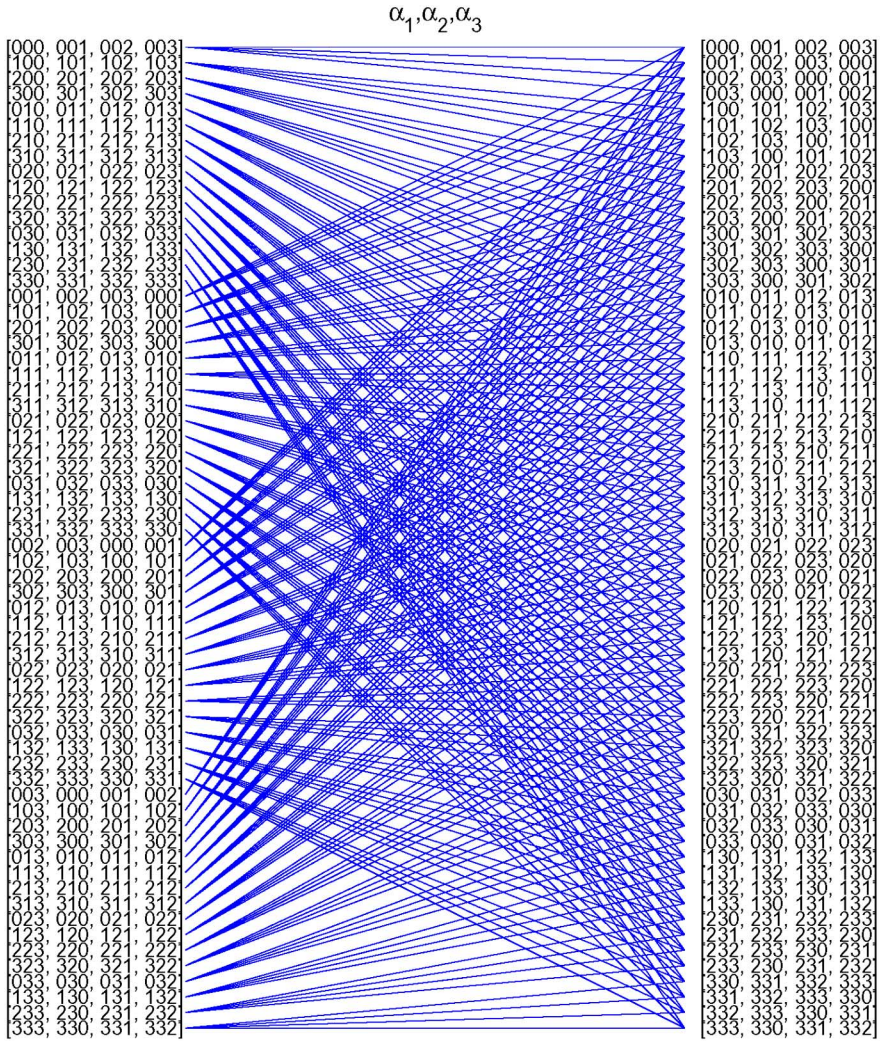


Fig. 14. The optimal 64-states trellis corresponding to the generators $g_1(D) = D, g_2(D) = D^2$, and $g_3(D) = 1 + D^3$. Labels on the left are outgoing from each state clockwise, labels on the right are incoming counterclockwise.

[21]. For our purposes we will use Construction A as means to handle the set partitioning and to bit-label the lattice points within a finite constellation.

As an example, let us consider a two-dimensional integer lattice $\mathbb{Z}^2$, depicted in Fig. 15. In such a lattice, the *checkerboard lattice* D_2 is a sublattice of $\mathbb{Z}^2$ containing all integer vectors (x, y) such that $x+y$ is even. Using the *repetition code* of length two $C = \{(00), (11)\}$ we write

$$D_2 = 2\mathbb{Z}^2 + C = [2\mathbb{Z}^2 + (00)] \bigcup [2\mathbb{Z}^2 + (11)]$$

This is illustrated in Fig. 15, where the squares denote the D_2 lattice that is the union of the $2\mathbb{Z}^2$ lattice (light squares) and its translate (dark squares).

Similarly, given the *universe code* $C_0 = (2, 2, 1) = \{(00), (01), (10), (11)\}$, we can write

$$\mathbb{Z}^2 = 2\mathbb{Z}^2 + C_0$$

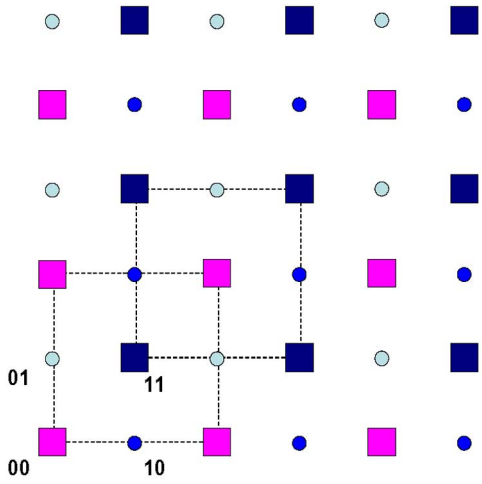


Fig. 15. Example of Construction A and set partitioning of $\mathbb{Z}^2$.

Given the linear code C, the *dual code* $C^{\perp}$ is defined such that $C \oplus C^{\perp} = C_0$, i.e., all the binary sums of a codeword

Authorized licensed use limited to: University of South Australia. Downloaded on November 23, 2008 at 22:42 from IEEE Xplore. Restrictions apply.

from C with a codeword from $C^{\perp}$ yield all the universe codewords. In our example, $C = \{(00),(11)\}$ has a dual code $C^{\perp} = \{(00),(01)\}$.

Linearity of the codes is related to the additive group structure and enables to interpret codes and subcodes as groups and subgroups. In turn, this lets us define a *quotient group* between a code and its subcode.

For example, given that $C \subset C_0$ we can write the quotient group as the set of two cosets of the subgroup C, i.e., $C_0/C = \{C + (00), C + (01)\}$.

A well-known property of Abelian groups tells us that the quotient group has itself a group structure. The quotient group operation $\oplus$ between two cosets is defined as

$$(C + \boldsymbol{c}_1) \oplus (C + \boldsymbol{c}_2) = C + (\boldsymbol{c}_1 + \boldsymbol{c}_2).$$

This implies that the quotient group is isomorphic to the so called *quotient code* denoted by $[C_0/C]$ and defined as the set of all the *coset leaders*. If C_0 is the universe code then the quotient code coincides with the dual code, i.e.,

$$[C_0/C] = C^{\perp} \tag{57}$$

In our example $[C_0/C] = \{(00),(01)\}$.

Let us consider a lattice Λ_0 and sublattice $\Lambda \subset \Lambda_0$. Thanks to the group structure of lattices, we can define the *quotient lattice* Λ_0/Λ as the set of all distinct translates (or cosets) of Λ, i.e.,

$$\Lambda_0/\Lambda = \{\Lambda + \boldsymbol{x}_i\} \tag{58}$$

where $\boldsymbol{x}_i$ are the translation vectors or coset leaders. Let $[\Lambda_0/\Lambda]$ denote the set of all the coset leaders then we write

$$\Lambda_0 = \Lambda + [\Lambda_0/\Lambda]. \tag{59}$$

If C_0 and C are the corresponding binary codes defined by Construction A, we have the following group isomorphism:

$$C_0/C \sim \Lambda_0/\Lambda. \tag{60}$$

Note that the quotient group defines a *partition* of C_0 into disjoint cosets of the same size $N_c = |C_0/C|$, where $|\cdot|$ denotes the cardinality of the set. Thanks to the above isomorphism, the *index* of the sublattice in the lattice is finite, i.e., $|\Lambda_0/\Lambda| = N_c$. Considering the fundamental volume of a lattices defined as $\mathrm{vol}(\Lambda) = \det(MM^T)^{1/2}$, where M is the lattice generator matrix, we have $\mathrm{vol}(\Lambda)/\mathrm{vol}(\Lambda_0) = N_c$.

Consider the sequence of nested lattices $2\mathbb{Z}^n \subseteq \Lambda \subset \Lambda_0 \subseteq \mathbb{Z}^n$. Each coset of the quotient lattice can be identified by a coset leader which is related to the quotient code as follows:

$$[\Lambda_0/\Lambda] \bmod 2 = [C_0/C] \quad \text{and} \quad [\Lambda/2\mathbb{Z}^n] \bmod 2 = C. \tag{61}$$

This is due to the fact that the lattice $2\mathbb{Z}^n$ is obtained by Construction A with the $(n,0)$ code, containing only the all-zero codeword. The partitions of the basic lattice Λ_0 can be written as

$$\Lambda_0 = \Lambda + [\Lambda_0/\Lambda] = \Lambda + [C_0/C]. \tag{62}$$

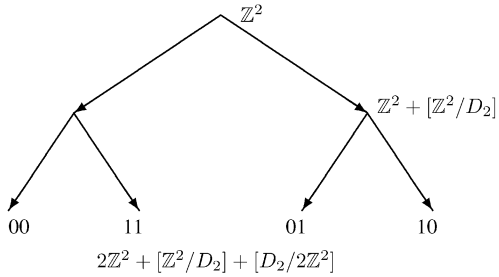


Fig. 16. The two-way partition tree of $\mathbb{Z}^2$.

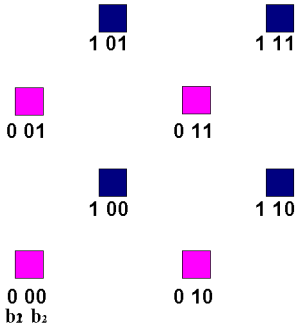


Fig. 17. Labeling the finite constellation carved from D_2.

In our example, we first partition $\mathbb{Z}^2$ into two cosets: the sublattice D_2 and its translate $D_2 + (01)$ (squares and circles in Fig. 15, respectively)

$$\mathbb{Z}^2 = D_2 + C^{\perp} = D_2 + [\mathbb{Z}^2/D_2].$$

The number of partitions equals to the index of the sublattice D_2 in $\mathbb{Z}^2$ and equals $N_c = |C^{\perp}| = 2$. We can further partition each coset by partitioning D_2 into two cosets. The sequence of nested lattices $\mathbb{Z}^2 \supset D_2 \supset 2\mathbb{Z}^2$ induces a partition chain

$$\mathbb{Z}^2 = 2\mathbb{Z}^2 + C^{\perp} + C = 2\mathbb{Z}^2 + [\mathbb{Z}^2/D_2] + [D_2/2\mathbb{Z}^2]$$

which can be represented by the *two-level binary partition tree* in Fig. 16.

We observe how Construction A yields a simple bit labeling of a finite constellation $\mathcal{S} = \Lambda \cap \mathcal{B}$ carved from the infinite lattice with shaping region $\mathcal{B}$. In particular, since $\Lambda = 2\mathbb{Z}^n + C$, with $C = (n,k)$ generated by code generator matrix G, the constellation points are written as $\boldsymbol{x} = 2\boldsymbol{u} + \boldsymbol{c}$, with $2\boldsymbol{u} \in 2\mathbb{Z}^n \cap \mathcal{B}$ and $\boldsymbol{c} \in C$.

In order to label the constellation points $\boldsymbol{x}$, we form the bit label vector $\boldsymbol{b}$ as the concatenation of two parts $\boldsymbol{b}_2$ and $\boldsymbol{b}_3$, i.e., $\boldsymbol{b} = (\boldsymbol{b}_2, \boldsymbol{b}_3)$. The first part $\boldsymbol{b}_2$ has k bits and indexes the codeword $\boldsymbol{c} = \boldsymbol{b}_2 G$. The second part $\boldsymbol{b}_3$ labels the integer vectors $\boldsymbol{u}$, such that $2\boldsymbol{u} + \boldsymbol{c} \in \mathcal{B}$. Note that the number of bits in $\boldsymbol{b}_3$ depends on the size of $\mathcal{B}$. When $\mathcal{B}$ has a cubic shape, we can apply a Gray labeling to each component of $\boldsymbol{u}$.

For example, Fig. 17 shows the labeling of an eight-point constellation carved from D_2, where one bit is used to select one on the two codewords (00) and (11), while the other two bits to select one of the four points in $2\mathbb{Z}^2 \cap \mathcal{B}$.

Authorized licensed use limited to: University of South Australia. Downloaded on November 23, 2008 at 22:42 from IEEE Xplore. Restrictions apply.

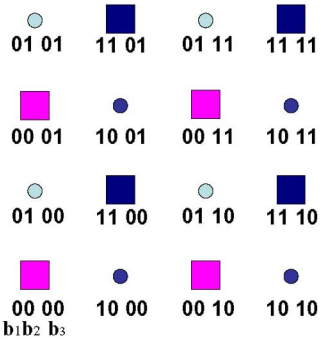


Fig. 18. Labeling the finite constellation carved from $\mathbb{Z}^2$ using the two level set partitioning.

Finally, we consider the labeling of the entire finite constellation carved from $\Lambda_0 \subseteq \mathbb{Z}^n$. In order to follow the partition into cosets induced by $\Lambda \subset \Lambda_0$, we use (62) to get

$$\Lambda_0 = \Lambda + [\Lambda_0/\Lambda] + [\Lambda/2\mathbb{Z}^n] = 2\mathbb{Z}^n + [C_0/C] + C. \quad (63)$$

In particular, we add $\boldsymbol{b}_1$ information bits, which are used to label the codewords of the quotient code $[C_0/C]$. So the final bit label is $\boldsymbol{b} = (\boldsymbol{b}_1, \boldsymbol{b}_2, \boldsymbol{b}_3)$.

Fig. 18 shows the labeling of the 16-QAM obtained by set partitioning corresponding to Fig. 15. The extra bit $\boldsymbol{b}_1$ selects one of the two codewords of the dual code (00) and (01), while $\boldsymbol{b}_2$ and $\boldsymbol{b}_3$ are the same as in Fig. 17. This labeling technique was first proposed by Ungerboeck and we can observe how the overall labeling is *not* a Gray labeling of the 16-QAM.

REFERENCES

[1] V. Tarokh, N. Seshadri, and A. R. Calderbank, "Space-time codes for high data rate wireless communications: Performance criterion and code construction," *IEEE Trans. Inf. Theory*, vol. 44, no. 2, pp. 744–765, Mar. 1998.

[2] S. M. Alamouti, "A simple transmit diversity technique for wireless communications," *IEEE J. Sel. Areas Communications*, vol. 16, no. 8, pp. 1451–1458, Oct. 1998.

[3] L. Zheng and D. N. C. Tse, "Diversity and multiplexing: A fundamental tradeoff in multiple-antenna channels," *IEEE Trans. Inf. Theory*, vol. 49, no. 5, pp. 1073–1096, May 2003.

[4] V. Tarokh, H. Jafarkhani, and A. R. Calderbank, "Space–time block codes from orthogonal designs," *IEEE Trans. Inf. Theory*, vol. 45, no. 5, pp. 1456–1467, Jul. 1999.

[5] M. O. Damen, K. Abed-Meraim, and J.-C. Belfiore, "Diagonal algebraic space-time block codes," *IEEE Trans. Inf. Theory*, vol. 48, no. 3, pp. 628–636, Mar. 2002.

[6] M. O. Damen, K. Abed-Meraim, and J.-C. Belfiore, "Transmit diversity using rotated constellations with Hadamard transform," in *Proc. 2000 IEEE Symp. Adaptive Systems for Signal Processing, Communications, and Control*, Lake Louise, AB, Canada, Oct. 2000, pp. 396–401.

[7] H. El Gamal and M. O. Damen, "Universal space–time codes," *IEEE Trans. Inf. Theory*, vol. 49, no. 5, pp. 1097–1119, May 2003.

[8] B. A. Sethuraman, B. S. Rajan, and V. Shashidhar, "Full-diversity, high-rate space-time block codes from division algebras," *IEEE Trans. Inf. Theory*, vol. 49, no. 10, pp. 2596–2616, Oct. 2003.

[9] J.-C. Belfiore, G. Rekaya, and E. Viterbo, "The golden code: A 2 × 2 full-rate space–time code with nonvanishing determinants," *IEEE Trans. Inf. Theory*, vol. 51, no. 4, pp. 1432–1436, Apr. 2005.

[10] P. Elia, K. R. Kumar, S. A. Pawar, P. V. Kumar, and H.-F. Lu, "Explicit space-time codes that achieve the diversity-multiplexing gain tradeoff," in *Proc. IEEE Int. Symp. Information Theory*, Adelaide, Australia, Sep. 2005, pp. 896–900.

[11] E. Viterbo and J. Boutros, "A universal lattice code decoder for fading channels," *IEEE Trans. Inf. Theory*, vol. 45, no. 5, pp. 1639–1642, Jul. 1999.

[12] H. Jafarkhani and N. Seshadri, "Super-orthogonal space–time trellis codes," *IEEE Trans. Inf. Theory*, vol. 49, no. 4, pp. 937–950, Apr. 2003.

[13] A. R. Calderbank and N. J. Sloane, "New trellis codes based on lattices and cosets," *IEEE Trans. Inf. Theory*, vol. IT-33, no. 2, pp. 177–195, Mar. 1987.

[14] G. Ungerboeck, "Trellis coded modulation with redundant signal sets. Part II: State of the art," *IEEE Commun. Mag.*, vol. 25, no. 2, pp. 12–21, Feb. 1987.

[15] G. D. Forney, Jr., "Coset codes. I. Introduction and geometrical classification," *IEEE Trans. Inf. Theory*, vol. 34, no. 5, pp. 1123–1151, Sep. 1988.

[16] G. D. Forney, Jr., "Coset codes. II. Binary lattices and related codes," *IEEE Trans. Inf. Theory*, vol. 34, no. 5, pp. 1152–1187, Sep. 1988.

[17] F. Oggier and E. Viterbo, "Algebraic number theory and code design for Rayleigh fading channels," *Found. Trends in Commun. and Inf. Theory*, vol. 1, pp. 333–415, 2004.

[18] D. Champion, J.-C. Belfiore, G. Rekaya, and E. Viterbo, "Partitionning the Golden code: A framework to the design of space-time coded modulation," in *Proc. Canadian Workshop on Information Theory*, Montreal, QC, Canada, Jun. 2005.

[19] E. Biglieri, *Coding for Wireless Channels*. New York: Springer-Verlag, 2005.

[20] J. Rotman, *An Introduction to the Theory of Groups*. New York: Springer-Verlag, 1994.

[21] J. H. Conway and N. J. A. Sloane, *Sphere Packings, Lattices and Groups*. New York: Springer-Verlag, 1992.

[22] H. Lütkepolhl, *Handbook of Matrices*. Chichester, U.K.: Wiley, 1996.

[23] F. J. MacWilliams and N. J. A. Sloane, *The Theory of Error-Correcting Codes*. Amsterdam, The Netherlands: North-Holland, 1977.

Authorized licensed use limited to: University of South Australia. Downloaded on November 23, 2008 at 22:42 from IEEE Xplore. Restrictions apply.